0013-7227/93/1325-2024$03.00/0
Endocrinology

Vol. 132, No. 5
Printed in U.S.A.

Analysis of Parathyroid Hormone's Principal Receptor-Binding Region by Site-Directed Mutagenesis and Analog Design

THOMAS J. GARDELLA*, ANDREW K. WILSON, HENRY T. KEUTMANN, ROBERT OBERSTEIN, JOHN T. POTTS, JR., HENRY, M. KRONENBERG, AND SAMUEL R. NUSSBAUM

Endocrine Unit, Masssachusetts General Hospital and Harvard Medical School, Boston, Massachusetts 02114

ABSTRACT

Previous deletion studies established that the 25–34 region of PTH is important for receptor binding. We used oligonucleotide-directed mutagenesis to generate 47 different mutations in this region of human (h) PTH-(1–84) and evaluated cAMP-stimulating activity in ROS 17/2.8 cells. The hydrophobic residues Leu^{24} and Leu^{28} stood out as mutationally intolerant sites, while neighboring polar residues were comparatively tolerant. A series of synthetic PTH analogs was designed to test these residues further. The affinity of [Tyr^{34}]hPTH-(1–34)NH_2 for ROS 17/2.8 cells [dissociation constant (K_d), ~5 nM)] was dramatically reduced by the substitution of either Leu^{24} or Leu^{28} with Glu (K_d, ~20,000 and 8,000 nM, respectively). The Val^{31}→Glu substitution also sharply reduced affinity (K_d, ~200 nM). In contrast, the nearby charge-reversing change of Asp^{30}→Lys had no effect on binding affinity (K_d, ~5 nM). Similar effects were observed in the opossum kidney cell line. The binding of [Tyr^{34}]hPTH-(15–34)NH_2 to ROS 17/2.8 and opossum kidney cells (K_d, ~10 μM) was abolished by Glu substitutions at position 24, 28, or 31; the Lys^{30} change was without effect. These results suggest that the adverse effects of the Glu substitutions on receptor binding are not due purely to the disruption of tertiary interactions with the 1–14 region. Circular dichroism spectroscopy indicated that the substitutions do not affect local helical structure. The data suggest that Leu^{24}, Leu^{28}, and Val^{31} contribute important receptor-binding interactions and are consistent with the hypothesis that an amphipathic α-helix in the carboxy-terminal region of PTH-(1–34) is involved in receptor binding. (*Endocrinology* **132:** 2024–2030, 1993)

THE INFORMATION required for high affinity binding of PTH to bone and kidney cell receptors is contained within the biologically active 1–34 region (1). The amino-terminus of PTH is essential for triggering the adenylate cyclase response pathway (2, 3), but it also contributes modestly to receptor-binding affinity. In addition to a nearly complete loss of cAMP agonism, the deletion of residues 1–6 is accompanied by an approximately 100-fold decrease in receptor-binding affinity (4–7). The major component of PTH receptor-binding affinity, however, appears to be determined by residues in the carboxy-terminal portion of the 1–34 fragment. Deletion of residues 28–34 causes at least a 1000-fold reduction in binding affinity (5). Furthermore, PTH-(25–34) displays weak, but detectable, receptor binding affinity (K_d, ~100 μM) (5). In contrast, no evidence for receptor interaction has been obtained for amino-terminal fragments shorter than PTH-(1–27) (3, 8). Based on these observations, the 25–34 region has been called the hormone's principal receptor-binding domain (5).

The carboxy-terminal region of the PTH-(1–34) fragment is highly conserved in evolution. Among the known mammalian PTH sequences, residues 23–34 are invariant. This 12-residue sequence of the mammalian hormone diverges only slightly from the corresponding sequence of the chicken hormone, with differences occurring only at positions 25, 26, 33, and 34 (9). Interestingly, the 1–34 fragment of PTH-related peptide (PTHrP) binds to the same receptor site as PTH (10–12). While the 1–13 regions of hPTHrP and hPTH are identical at eight sites, their 14–34 regions share only three identities: Arg^{20}, Leu^{24}, and His^{32} (13). Therefore, it is intriguing that fragments of PTH and PTHrP lacking the conserved 1–13 sequence bind with equivalent affinities to the same receptor site (14, 15). This result may be an indication that the two peptides adopt similar conformations when bound to the receptor. Recent nuclear magnetic resonance imaging (NMR) analyses of PTH-(1–34) (16) and PTHrP(1–34) (17), however, suggest that in certain solvents the carboxy-terminal regions of the two peptides are structurally distinct. In 10% trifluroethanol, residues 17–28 of PTH are α-helical, while in water, this region of PTHrP is ordered, but nonhelical. Whether these conformational differences are maintained in the receptor-bound state is currently unkown.

A greater understanding of PTH/PTHrP conformation and receptor interaction will depend on such biophysical analyses as well as functional studies that use modified ligands to identify critical amino acids. As part of our efforts to identify the sites in PTH that determine receptor-binding affinity, we conducted a mutational analysis of the hormone's conserved 23–35 region. We first screened a panel of randomly generated hPTH-(1–84) mutants for biological activity and then designed and characterized a series of synthetic analogs with which to further explore the role of selected residues. The data suggest that certain hydrophobic residues in the target

Received November 15, 1992.
* To whom requests for reprints should be addressed.

region that are conserved in PTH and PTHrP are important for PTH receptor binding.

Materials and Methods

Cell culture

Cell lines were maintained in a humidified atmosphere containing 95% air-5% CO_2 in 250-ml culture flasks (75 cm^2). Cells were subcultured into 24-well plates before DNA transfection or biological activity assays. COS-7 and OK cells were cultured in Dulbecco's Modified Eagle's Medium (Mediatech, Washington DC) supplemented with 10% fetal bovine serum (Hyclone Laboratories, Logan, UT); ROS 17/2.8 cells were cultured in Ham's F-12 medium (Mediatech) supplemented with 5% fetal calf serum.

PTH mutagenesis

Mutations were introduced into the hPTH-(1–84) cDNA sequence carried on the plasmid pCDM-PTH-1 (18) by site-directed mutagenesis (19). Three separate pools of partially degenerate oligonucleotides were used to mutagenize codons 23–27, 28–31, and 32–35. Phagemid supernatents from approximately 600 independent transformants of the *E. coli* strain Fg2 were screened for mutations by slot blot hybridization, using a ^{32}P-labeled wild-type oligonucleotide spanning the target region as the probe. Sequence analysis of single stranded plasmid DNA obtained from the resulting 173 nonhybridizing mutants revealed 47 differrent single residue substitutions. The remaining nucleotide changes resulted in multiple amino acid substitutions, termination codons, or the wild-type polypeptide sequence.

Human PTH-(1–84) expression

Double stranded plasmid DNA of each mutant was introduced into COS-7 cells by diethylaminoethyl-dextran transfection (20). Three to 5 days later, the conditioned media containing secreted hormone were harvested, and PTH levels were quantified by an immunoradiometric assay (IRMA) specific for intact hPTH-(1–84) (Nichols Institute, San Jaun Capistrano, CA). The average hPTH-(1–84) concentration in these media was 7.0 ± 0.5 nM. Media containing less than 2 nM PTH were not included in the study. The PTH concentration in these media was also measured using a RIA directed against the 44–68 region of hPTH (Nichols). The results of the midregion RIA agreed closely with those obtained by IRMA. The media were not specifically assayed for possible amino-terminal PTH fragments, the presence of which could lead to an overestimation of a mutant's biological activity. We recently showed, however, that COS cells transfected with pCDM-PTH-1 do not secrete amino-terminal PTH fragments in significant amounts (21).

Peptide synthesis

Derivatives of [Tyr^{34}]hPTH-(1–34)NH_2 and [Tyr^{34}]hPTH-(15–34)NH_2 were prepared by the solid phase procedure (22), using an Applied Biosystems model 430 peptide synthesizer (Foster City, CA). Peptides were purified by gel filtration and sequential HPLC. Amino acid composition, sequence analysis, and pulse desorption mass spectroscopy verified the authenticity of each peptide.

Competitive radioreceptor binding

Binding assays were performed as previously described (18). Briefly, ROS17/2.8 and OK cells were maintained in 24-well plates as confluent monolayers for 3–5 days before assay. Binding reactions (300 μl) contained binding buffer [50 mM Tris-HCl (pH 7.7), 100 mM NaCl, 5 mM KCl, 2 mM CaCl, 5% heat-inactivated horse serum, and 0.5% fetal bovine serum], an unlabeled PTH analog, and radiolabeled PTH (50,000 cpm), the latter two diluted in binding buffer. The tracer, ^{125}I-labeled [$Nle^{8,18}$,Tyr^{34}]bPTH-(1–34)NH_2 (2.2 × 10^6 mCi/mM), was prepared by chloramine-T iodination, using ^{125}INa (New England Nuclear, Boston, MA), and HPLC purified. After 4 h at 16 C, the binding mixture was removed, the cells were rinsed 3 times with 0.5 ml binding buffer and lysed with 0.5 ml 5 M NaOH, and the entire lysate was counted for γ-irradiation. Nonspecific binding and total binding were determined for each plate from triplicate wells containing 1 μM unlabeled [Tyr^{34}] hPTH-(1–34)NH_2 and no unlabeled PTH, respectively. The specific binding at each dose of ligand was expressed as a percentage of the total specific binding. Dissociation constants (K_d) were estimated from the binding curves.

Intracellular cAMP stimulation assays

Cells were cultured as they were for binding assays. For assay of hPTH-(1–84) mutants, the 24-well plates containing confluent ROS 17/2.8 cells were chilled on ice, cell monolayers were rinsed with cold binding buffer, and 200 μl cAMP assay buffer [Dulbecco's Modified Eagle's Medium containing 2 mM 3-isobutyl-1-methylxanthine, 1 mg/ml BSA, 35 mM HEPES-NaOH (pH 7.4), and 20 μg/ml ascorbic acid] and 100 μl conditioned COS cell medium containing an hPTH-(1–84) mutant were added. Plates were transferred to a 37 C incubator for 30 min. The buffer was then withdrawn, and the cells were lysed by adding 0.5 ml 50 mM HCl and freezing the plate on dry ice. The cAMP in the lysate was quantified by RIA (Biomedical Technologies, Inc., Reading, MA). Synthetic PTH-(1–34) analogs were assayed in a similar fashion, except that 100 μl binding buffer containing a diluted peptide were added in place of the COS cell medium. The cAMP response elicited by each PTH-(1–84) mutant was adjusted for the concentration of immunoreactive hPTH-(1–84) in the conditioned COS medium (determined by IRMA) and expressed as a percentage of the response elicited by the COS medium obtained from cells transfected with wild-type pCDM-PTH-1. Data from independent mutants with identical mutations were combined. Activities of hPTH-(1–34) analogs were expressed as a percentage of the maximum cAMP response attained with the parent peptide, [Tyr^{34}]hPTH-(1–34)NH_2.

Circular dichroism

Circular dichroism spectra were obtained with a Jasco J-500A spectropolarimeter (Easton, MD). Spectra were recorded in either TES [*N*-Tris-(hydroxymethyl)2-aminoethanesulfonic acid] buffer at pH 7.5 or in TES buffer containing 50% trifluoroethanol (TFE). Spectra were recorded between 180–260 nM at 25 C; the cuvette path length was 100 mm, and the concentration of petide in the cell ranged from 0.096–0.110 mg/ml, as determined by amino acid analysis. Estimations of secondary structure were made based on the method of Chen *et al.* (23).

Results

We used site-directed mutagenesis to randomly mutate residues 23–35 of hPTH-(1–84), expressed the mutants in COS-7 cells, and evaluated their biological activities in the rat osteosarcoma cell line ROS 17/2.8. The concentration of hPTH-(1–84) obtained from transfected COS cells (7 ± 0.5 nM) approximated the dose at which hPTH-(1–84) stimulates a half-maximal cAMP response in ROS 17/2.8 cells (24). Therefore, we could screen each mutant for function by treating ROS 17/2.8 cells directly with the conditioned COS medium and measuring the resulting increase in intracellular cAMP (Fig. 1). Several sites in the target region could tolerate a variety of mutations. At these sites, which included Lys^{26}, Lys^{27}, Gln^{29}, Asp^{30}, His^{32}, Asn^{33}, Phe^{34}, and Val^{35}, none of the changes reduced activity to below the detection limit of the assay (~2% the activity of the wild-type hormone), and many changes resulted in a fully active hormone. Two residues that appeared comparatively intolerant of mutation were Leu^{24} and Leu^{28}. None of the changes at these two sites

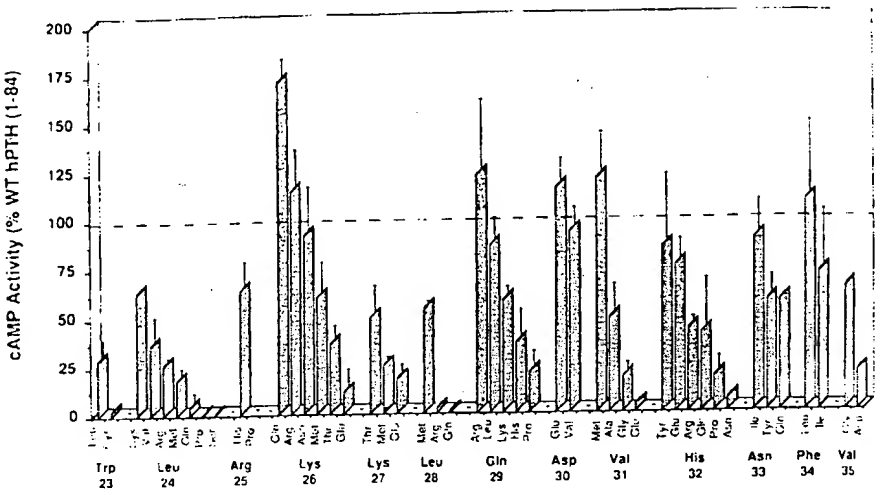

FIG. 1. Scanning mutagenesis of the 23–35 region of hPTH-(1–84). hPTH-(1–84) mutants were produced in COS-7 cells and screened for cAMP-stimulating activity in ROS 17/2.8 cells, as described in *Materials and Methods*. The activity of each mutant is expressed relative to the activity of the wild-type hPTH-(1–84) control, also produced in COS-7 cells. Values are the mean ± SEM of between 3–10 independent determinations.

resulted in full potentcy, and at least one change at each site abolished activity. Val^{31} displayed an intermediate level of mutational tolerance; the Met^{31} mutant was fully active, but the Glu^{31} and Gly^{31} mutants displayed only a weak cAMP response. It is difficult to gauge the mutational tolerance of some sites, such as Trp^{23} and Arg^{25}, because only two changes with varying effects were obtained. While the Cys^{23} and Pro^{25} mutants were inactive, the Leu^{23} and His^{25} mutants displayed partial activities.

One pattern that emerged from screening these mutants was that polar residues at the normally hydrophobic sites of Leu^{24}, Leu^{28}, and Val^{31} were not well tolerated. It has been postulated that the carboxy-terminal region of PTH-(1–34) could form an amphipathic α-helix which may be involved in function (25, 26). The finding that polar substitutions at the residues that form the major portion of the hydrophobic face of this putative helix (26) resulted in decreased biological activity led us to design [Tyr^{34}]hPTH-(1–34)NH_2 analogs with modifications that would further test the roles of these residues. Leu^{24}, Leu^{28}, and Val^{31} were individually replaced with a negatively charged glutamic acid residue. For comparison, we replaced the neighboring Asp^{30} residue with a positively charged lysine. Figure 2A shows that in ROS 17/2.8 cells, each of the Glu substitutions caused a dramatic reduction in binding affinity. The binding affinities of the Glu^{24}- and Glu^{28}-substituted analogs were reduced by factors of 4000 and 1600 (K_d, ~20,000 and 8,000 nM), respectively, relative to that of the parent peptide (K_d, ~5 nM). The affinity of the Glu^{31} analog was reduced by a factor of 40 (K_d, ~200 nM). In contrast, the nonconservative change of Asp→Lys at position 30 had no effect on receptor-binding affinity (K_d, ~5 nM). The effects of these substitutions on cAMP-stimulating activity in ROS 17/2.8 cells were in approximate proportion to their effects on receptor-binding affinity (Fig. 2C). The Glu^{24}, Glu^{28}, and Glu^{31} analogs were all very weak agonists, while the Asp^{30}→Lys-substituted peptide displayed a slight (3-fold) increase in cAMP-generating potency relative to that of the parent peptide.

The sequences of the PTH receptor cDNAs obtained from ROS 17/2.8 cells and opossum kidney (OK) cells reveal that the two receptors are 78% identical at the amino acid level (27, 28). Figure 2, B and D, shows that the above series of PTH(1–34) modifications caused effects on the ligand's interaction with the OK cell receptor which were similar to those observed with the structurally distinct ROS 17/2.8 cell receptor. As in ROS cells, the Glu^{24} substitution had the most dramatic effect on OK cell binding and reduced affinity by about 5,000-fold (K_d, ~10,000 nM) relative to that of the parent peptide (K_d, ~2 nM). The Glu^{28} and Glu^{31} substitutions also reduced binding affinity for OK cells, although their effects on OK cell binding were slightly less severe than they were on ROS 17/2.8 cell binding. In OK cells, the Glu^{28} and Glu^{31} substitutions reduced binding affinity 200- and 10-fold (K_d, ~400 and 20 nM), respectively, relative to that of the parent peptide. As in ROS 17/2.8 cells, the Lys^{30} substitution had no effect on OK cell binding affinity. The cAMP-stimulating activities of these analogs in OK cells were in approximate proportion to their receptor-binding affinities (Fig. 2D). The ability of the Glu^{31} and Glu^{28} analogs to stimulate a full cAMP response in OK cells, but not in ROS 17/2.8 cells, is presumably a reflection of their slightly higher affinity for the OK cell receptor. In general, the modifications in this series of analogs cause similar effects on both ROS 17/2.8 and OK cell receptor interactions.

A possible model to explain the substantial reduction in binding affinities associated with the glutamate substitutions is that they disrupt important conformational interactions. If the adverse effects of the Glu substitutions are due solely to the disruption of tertiary interactions with the 1–14 region, then they should have no effect on the binding of the PTH-(15–34) fragment. To investigate such possible intramolecular interactions, we introduced the same series of substitutions into the PTH-(15–34) fragment and determined their effects on receptor binding. As shown in Fig. 3, the parent peptide, [Tyr^{34}]hPTH-(15–34)NH_2, bound to the ROS 17/2.8 and OK cell receptors with weak, but detectable, affinity (K_d, ~10 μM). As with the intact peptide, the Asp^{30}→Lys substitution had no effect on the binding of PTH-(15–34) to either the ROS 17/2.8 or OK cell receptor. Each of the three glutamate substitutions abolished the ability of the 15–34

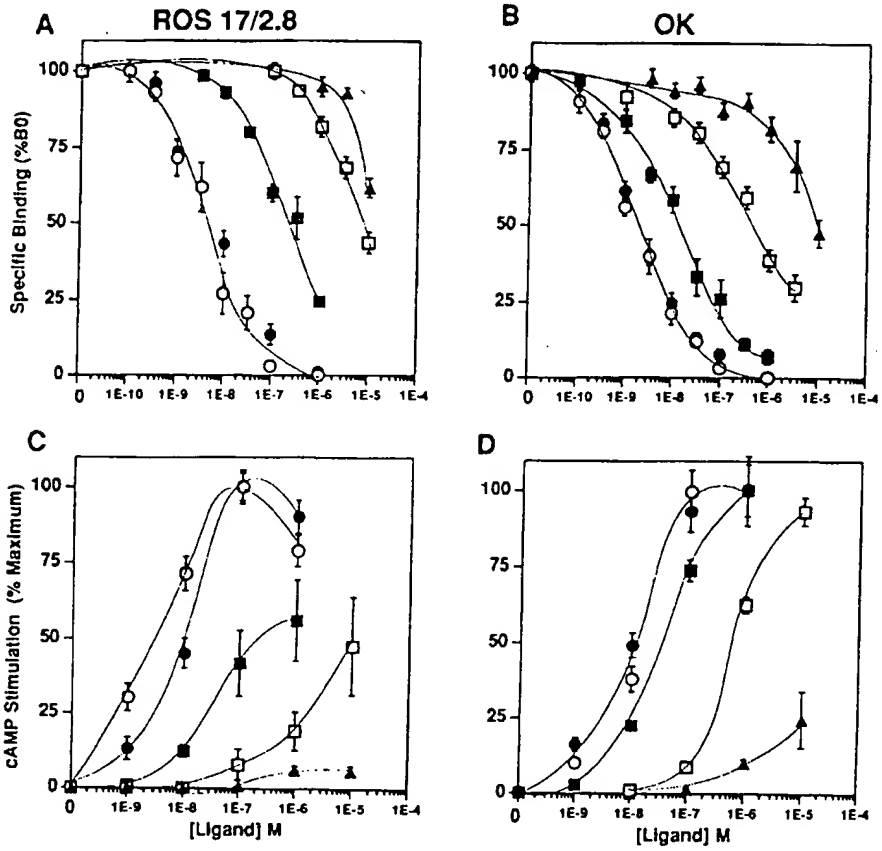

FIG. 2. Activities of hPTH-(1–34) analogs. Analogs of [Tyr^{34}]hPTH-(1–34)NH_2 [PTH-(1–34)] having Leu^{24}, Leu^{28}, and Val^{31} individually substituted with glutamic acid were chemically synthesized. In a fourth analog, Asp^{30} was substituted with lysine. A and B show the inhibition of receptor binding of ^{125}I-labeled [Nle^{8,18},Tyr^{34}]bPTH-(1–34)NH_2 in ROS 17/2.8 and OK cells, respectively. C and D show the cAMP-stimulating activities of the PTH-(1–34) analogs in ROS 17/2.8 and OK cells, respectively. Cells were treated as described in *Materials and Methods*. ●, PTH-(1–34); ○ [Lys^{30}]PTH-(1–34); ■, [Glu^{31}]PTH-(1–34); □, [Glu^{28}]PTH-(1–34); ▲, [Glu^{24}] PTH-(1–34). Values are the mean ± SEM of data from three to five (A and B) or two (C and D) experiments, each performed in triplicate.

fragment to bind to the ROS 17/2.8 and OK cell receptors. Although these results do not exclude the possibility that the 1–14 and 15–34 regions of PTH interact, they suggest that the negative effects of the carboxy-terminal Glu substitutions on receptor binding are not based purely on the disruption of such interactions.

To investigate possible effects on secondary structure, each of the analogs was evaluated by circular dichroism (CD) spectroscopy. Spectra were recorded of peptides dissolved in both aqueous buffer and buffer containing 50% TFE, a solvent that induces helical structure in certain peptides (29). As shown in Fig. 4, the CD spectra of hPTH-(15–34) shows a negative deflection in mean residue ellipticity (θ) at 220 nM (n-π^* transition) as well as a partial shift in a second minimum (π-π transition) from 190 toward 210 nM. These features are indicative of α-helical structure and correspond to a calculated helical content of 35%. This helical profile is enhanced by the presence of TFE. In this solvent system, the helical content of the peptides increases to 60%. The spectra of the Glu^{24}-substituted PTH-(15–34) peptide, obtained in either aqueous solvent or 50% TFE, were comparable to those of the unsubstituted parent peptide (Fig. 4). Equivalent results were obtained for each of the other analogs in the 15–34 series. Similar percent helical contents were obtained for each of the analogs in the 1–34 series. These results suggest that the amino acid substitutions that we have introduced into the hormone's principal binding domain do not induce dramatic alterations in secondary structure in either the shortened or full-length peptide.

Discussion

The mutational analysis presented here extends earlier deletion studies which showed that the 25–34 region of PTH contains important receptor binding determinants. The screening of 47 different hPTH-(1–84) mutants with changes in this region led us to focus on three residues: Leu^{24}, Leu^{28}, and Val^{31}. The mutational intolerance of these residues, paricularly Leu^{24} and Leu^{28}, strongly suggests that they are critical for optimal PTH activity. The biochemical basis of this functional significance is at this point a matter of speculation. Several observations, however, suggest that these residues contribute important receptor binding interactions.

By comparing the effects of modifications on the binding affinity of intact PTH-(1–34) to their effects on the binding of the PTH-(15–34) fragment we were able to investigate possible long range tertiary interactions between the modified site and the 1–14 region. Such interactions were considered plausible for several reasons. The NMR spectra of PTHrP-(1–34) revealed several cross-peak nuclear Overhauser effects involving the residue pairs of Val^2 and Ile^{31}, Leu^8 and Ile^{28}, and Lys^{13} and Leu^{24} (17). In the structural model

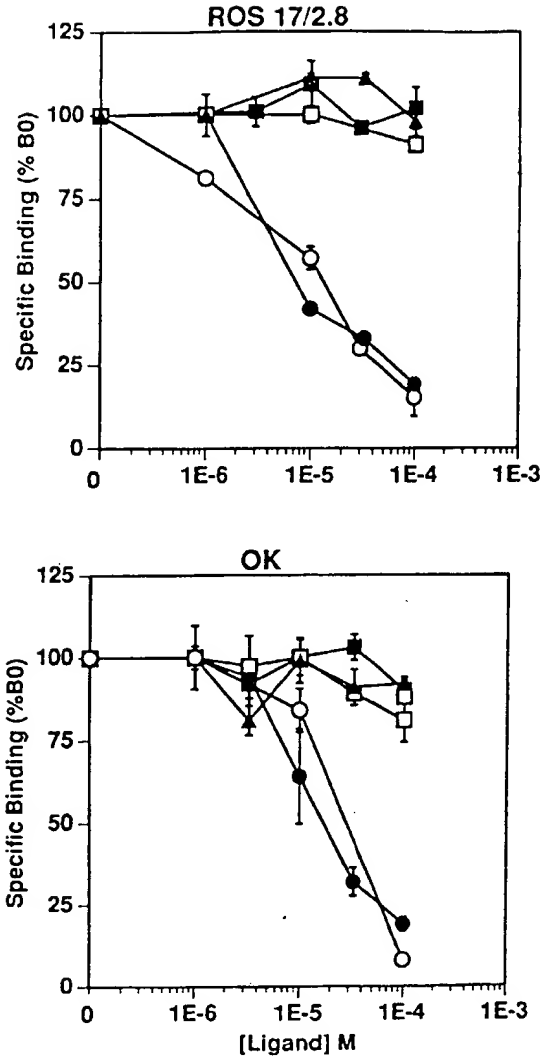

FIG. 3. Receptor binding of 15–34 fragments. The same substitutions shown in Fig. 2 were introduced into the [Tyr^{34}]hPTH-(15–34)NH_2 fragment [PTH-(15–34)]. *Top and bottom panels* show the inhibition of receptor binding of ^{125}I-labeled [Nle^{18,8},Tyr^{34}]bPTH-(1–34)NH_2 in ROS 17/2.8 and OK cells, respectively. ●, [Tyr^{34}]hPTH-(15–34); ○, [Lys^{30}]PTH-(15–34); ■, [Glu^{31}]PTH-(15–34); □, [Glu^{28}]PTH-(15–34); ▲, [Glu^{24}]PTH-(15–34). Values are the mean ± SEM of data from one representative experiment, performed in triplicate.

of PTHrP-(1–34) derived from these data, the carboxy- and amino-terminal domains are folded tightly together (17). Although cross-peak nuclear Overhauser effects were not observed in the NMR spectra of PTH-(1–34) (16), interactions between its amino- and carboxy-terminal portions have been proposed in conformational modeling studies (30–32). Our data showing that the Glu substitutions at positions 24, 28, and 31 diminish the binding affinity of both PTH-(1–34) and PTH-(15–34) suggest that the primary roles of the normal residues at these positions are not based purely on interactions with the 1–14 region. Other as yet untested residues in the 15–34 region, such as the conserved arginine at position 20, could be involved in maintaining conformational stability. It remains possible that Leu^{24}, Leu^{28}, and Val^{31} do participate in long range tertiary interactions with the 1–14 region, but these would appear to be in addition to their more local effects.

The results of our circular dichroism analysis suggest that a portion of the 15–34 region is α-helical. This finding is consistent with the CD analysis of Neugebauer *et al.* (26), which indicates that the PTH-(19–34) fragment contains substantial helical structure, and with the NMR study of Klaus *et al.* (16), which suggests that residues 17–28 of PTH-(1–34) form an α-helix. We found that in either water or 50% TFE, each of the Glu substitutions had little or no effect on the CD spectra of the PTH-(1–34) or PTH-(15–34) peptides. Although minor perturbations of structure may not be detected by CD spectroscopy, these results suggest that the Glu substitutions do not significantly alter secondary structure. This finding may in part be attributed to the high helix-forming propensity of glutamic acid (33); however, we point out that we have not defined the exact residues that determine the inferred 15–34 region α-helix. Whether this presumed helix is maintained in the receptor-bound state is also unkown, but the significant reduction in biological activity caused by proline substitutions at positions 24, 25, and 29 is consistent with this notion. If this putative helix is important for establishing or maintining receptor-binding affinity, then the binding defect associated with the glutamate substitutions could result from a steric or electrostatic incompatibility between the carboxylate side-chains and the ligand-binding surface of the receptor.

Neugebauer and co-workers (26) recently showed that phospholipid induces helical structure in PTH-(19–34), a response typical of amphipathic peptides. The increase in mean residue elipticity that we observed when TFE was added to the PTH fragments is also a characteristic response of peptides with potential amphipathic character (29). Theoretical helical wheel projection of the 21–34 region of PTH indicates that Leu^{24}, Leu^{28}, and Val^{31} would align to the hydrophobic face of this putative helix (26). Possible mechanisms by which the hydrophobic surface of such a helix could enhance receptor-binding affinity may involve nonspecific interactions with the cell membrane or specific interactions with a hydrophobic component of the receptor. Such mechanisms have been proposed for other peptide ligands possessing amphipathic potential (34). Our finding that other hydrophobic mutations at positions 24 and 28 (*e.g.* Val^{24}, Met^{24}, and Met^{28}) caused partial reductions in activity suggests that hydrophobicity *per se* is not sufficient for optimal receptor binding. Our data are, thus, consistent with the hypothesis that the hydrophobic residues in the carboxy-terminal region of PTH contribute important receptor-binding interactions.

Most mutations at the polar residues in the carboxy-terminal region of hPTH-(1–84) (*i.e.* Lys^{26}, Lys^{27}, Gln^{29}, Asp^{30}, and His^{32}) caused only marginal effects on activity, and the charge-reversing change of Asp→Lys at position 30 of hPTH-(1–34) had no effect on binding affinity. Results

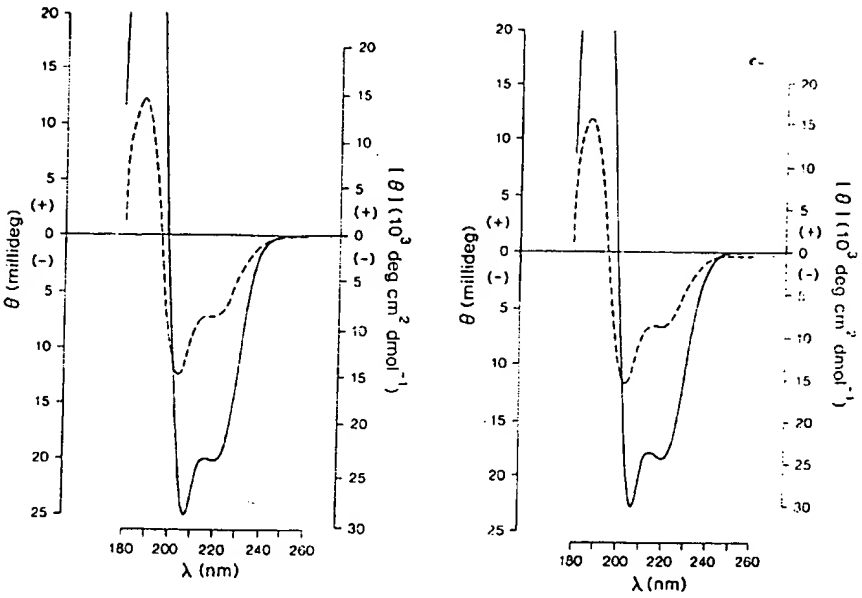

FIG. 4. Circular dichroism spectra of PTH-(15–34) fragments. Spectra are of [Tyr^{34}]hPTH-(15–34)NH_2 (*left panel*) and [Glu^{24},Tyr^{34}]hPTH-(15–34)NH_2 (*right panel*). Peptides were dissolved in either aqueous buffer (TES; - - -) or TES buffer containing 50% TFE (—-).

from other studies also suggest that these residues are mutationally tolerant. Reppe and co-workers (35) showed that a recombinant hPTH-(1–84) variant with a Lys^{26}→Gln substitution was fully active in assays of adenylate cyclase, hypercalcemia induction in parathyroidectomized rats, and stimulation of bone resorption in mouse calvaria. Biotinylation of Lys^{26} or Lys^{27} of [Nle^{8,18},Tyr^{34}]bPTH-(1–34)NH_2 had no effect on binding affinity (36). The peptides with the changes of His^{32} to Arg, [Arg^{32},Tyr^{34}]bovine (b) PTH-(1–34)NH_2, and Asp^{30} to Tyr, [Ile^{28},Tyr^{30,34}]bPTH-(1–34) were also fully active in adenylate cyclase and receptor binding assays (37). These data are consistent with the notion that the polar face of the putative carboxy-terminal helix has a more limited role in PTH receptor-binding than the opposite apolar face. However, since we found that certain substitutions at some of the polar sites, such as Lys^{26}→Glu or His^{32}→Asn, cause partial reductions in activity, a functional role for the polar residues should not be excluded. Furthermore, the activation of other signaling pathways, such as the intracellular Ca/protein kinase-C pathway and the proliferative response found in chick chondrocytes, requires the carboxy-terminal region of PTH-(1–34) (38–40). The precise role of both the polar and hydrophobic residues in stimulating these responses remains to be determined.

Whether the binding of PTH-(1–34) and PTHrP(1–34) to the same receptor occurs through similar arrays of receptor-ligand interactions is an intriguing question. Although the amino acid sequences of the carboxy-terminal regions of the two peptides are quite different, hydrophobicity is preserved at positions 24, 28, and 31. It will be interesting to see whether this region of PTHrP displays the same pattern of mutational tolerance as that observed here for PTH.

The functional analysis of novel PTH analogs, generated through peptide chemistry or site-directed mutagenesis, can provide important clues to the critical residues involved in hormone action. Such functional studies should provide a valuable complement to biophysical experiments involving NMR and x-ray crystallography. Taken together, the information gained from these approaches should lead to new insights into how PTH and PTHrP interact with a common receptor.

References

1. **Potts Jr JT, Tregear GW, Keutmann HT, Niall HD, Sauer R, Deftos LJ, Dawson BF, Hogan ML, Aurbach GD** 1971 Synthesis of a biologically active N-terminal tetratriacontapeptide of parathyroid hormone. Proc Natl Acad Sci USA 68:63–67
2. **Goltzman D, Peytremann A, Callahan E, Tregear GW, Potts JT Jr** 1975 Analysis of the requirements for parathyroid hormone action in renal membranes with the use of inhibiting analogues. J Biol Chem 250:3199–3203
3. **Tregear GW, Van Rietschoten J, Greene E, Keutmann HT, Niall HD, Reit B, Parsons JA, Potts Jr JT** 1973 Bovine parathyroid hormone: minimum chain length of synthetic peptide required for biological activity. Endocrinology 93:1349–1353
4. **Goldman ME, Chorev M, Reagan JE, Nutt RF, Levy JJ, Rosenblatt M** 1988 Evaluation of novel parathyroid hormone analogs using a bovine renal membrane receptor binding assay. Endocrinology 123:1468–1475
5. **Nussbaum SR, Rosenblatt M, Potts Jr JT** 1980 Parathyroid hormone/renal receptor interactions: demonstration of two receptor-binding domains. J Biol Chem 255:10183–10187
6. **Rosenblatt M, Segre GV, Tyler GA, Shepard GL, Nussbaum SR, Potts Jr JT** 1980 Identification of a receptor-binding region in parathyroid hormone. Endocrinology 107:545–5507
7. **Horiuchi N, Holick MF, Potts Jr JT, Rosenblatt M** 1983 A parathyroid hormone inhibitor *in vivo*: design and biologic evaluation of a hormone analog. Science 220:1053–1055
8. **Rosenblatt M** 1981 Parathyroid hormone: chemistry and structure-activity relations. In: Ioachim HL (ed) Pathobiology Annual. Raven Press, New York, vol 11:53–84
9. **Khosla S, Demay M, Pines M, Hurwitz S, Potts Jr JT, Kronenberg HM** 1988 Nucleotide sequence of cloned cDNAs encoding chicken preproparathyroid hormone. J Bone Mineral Res 3:689–698
10. **Jüppner H, Abou-Samra AB, Uneno S, Gu WX, Potts Jr JT, Segre GV** 1988 The parathyroid hormone-like peptide associated with humoral hypercalcemia of malignancy and parathyroid hormone

bind to the same receptor on the plasma membrane of ROS 17/2.8 cells. J Biol Chem 263:8557–8560
11. Kemp BE, Mosely JM, Rodda CP, Ebeling PR, Wettenhall REH, Stapleton D, Diefenbach-Jagger H, Ure F, Michelangali VP, Simmons HA, Raisz LG, Martin TJ 1987 Parathyroid hormone-related protein of malignancy: active synthetic fragments. Science 238:1568–1570
12. Nissenson RA, Diep D, Strewler GJ 1988 Synthetic peptides comprising the amino-terminal sequence of a parathyroid hormone-like protein from human malignancies. Binding to parathyroid hormone receptors and activation of adenylate cyclase in bone cells and kidney. J Biol Chem 263:12866–12871
13. Suva LJ, Winslow GA, Wettenhall RE, Hammonds RG, Moseley JM, Diefenbach JH, Rodda CP, Kemp BE, Rodriguez H, Chen EY, Hudson PJ, Martin TJ, Wood WI 1987 A parathyroid hormone-related protein implicated in malignant hypercalcemia: cloning and expression. Science 237:893–896
14. Abou-Samra A-B, Uneno S, Jüppner H, Keutmann H, Potts Jr JT, Segre GV, Nussbaum SR 1989 Non-homologous sequences of parathyroid hormone and the parathyroid hormone related peptide bind to a common receptor on ROS 17/2.8 cells. Endocrinology 125:2215–2217
15. Caulfield MP, McKee RL, Goldman ME, Duong LT, Fisher JE, Gay CT, DeHaven PA, Levy JJ, Roubini E, Nutt RF, Chorev M, Rosenblatt M 1990 The bovine renal parathyroid hormone (PTH) receptor has equal affinity for two different amino acid sequences: the receptor binding domains of PTH and PTH-related protein are located within the 14–34 region. Endocrinology 127:83–87
16. Klaus W, Dieckmann T, Wray V, Schomburg D, Wingender E, Mayer H 1991 Investigation of the solution structure of the human parathyroid hormone fragment (1–34) by ^{1}H NMR spectroscopy, distance geometry, and molecular dynamics calculations. Biochemistry 30:6936–6942
17. Barden JA, Kemp BE 1989 NMR study of a 34-residue N-terminal fragment of the parathyroid-hormone-related protein secreted during humoral hypercalcemia of malignancy. Eur J Biochem 184:379–394
18. Gardella TJ, Axelrod D, Rubin D, Keutmann HT, Potts Jr JT, Kronenberg HM, Nussbaum SR 1991 Mutational analysis of the receptor-activating region of human parathyroid hormone. J Biol Chem 266:13141–13146
19. Kunkel TA 1985 Rapid and efficient site-specific mutagenesis without phenotypic selection. Proc Natl Acad Sci USA 82:488–492
20. Seed B, Aruffo A 1987 Molecular cloning of the CD2 antigen, the T-cell erythrocyte receptor. Proc NAtl Acad Sci USA 84:3365–3369
21. Lim SK, Gardella TJ, Baba H, Nussbaum SR, Kronenberg HM 1992 The carboxy-terminus of parathyroid hormone is essential for hormone processing and secretion. Endocrinology 131:2325–2330
22. Barany G, Merrifield RB 1979 Solid phase peptide synthesis. In: Gross E, Meinhofer J (eds) The Peptides. Academic Press, New York, vol 2:1–284
23. Chen Y-H, Yang J-T, Chau K-H 1974 Determination of the helix and B form of proteins in aqueous solution by circular dichroism. Biochemistry 13:3350–3359
24. Gardella TJ, Rubin D, Abou-Samra AB, Keutmann HT, Potts Jr JT, Kronenberg HM, Nussbaum SR 1990 Expression of human parathyroid hormone-(1–84) in *Escherichia coli* as a factor X-cleavable fusion protein. J Biol Chem 265:15854–15859
25. Epand RM, Epand RF, Hui SW, He NB, Rosenblatt M 1985 Formation of water-soluble complex between the 1-34 fragment of parathyroid hormone and dimyristoylphosphotidyl choline. Int J Peptide Protein Res 25:594–600
26. Neugebauer W, Surewicz WK, Gordon HL, Somorjai RL, Sung W, Willick GE 1992 Structural elements of human parathyroid hormone and their possible relation to biological activities. Biochemistry 31:2056–2063
27. Abou-Samra AB, Jüppner H, Force T, Freeman M, Kong XF, Schipani E, Urena P, Richards J, Bonventre JV, Potts Jr JT, Kronenberg HM, Segre GV 1992 Expression cloning of a common receptor for parathyroid hormone and parathyroid hormone-related peptide from rat osteoblast-like cells: a single receptor stimulates intracellular accumulation of both cAMP and inositol triphosphates and increases intracellular free calcium. Proc Natl Acad Sci USA 89:2732–2736
28. Jüppner H, Abou-Samra A-B, Freeman M, Kong X-F, Schipani E, Richards J, Kolakowski Jr LF, Hock J, Potts Jr JT, Kronenberg HM, Segre GV 1991 A G protein-linked receptor for parathyroid hormone and parathyroid hormone-related peptide. Science 254:1024–1026
29. Lynch B, Kaiser ET 1988 Biological properties of two models of calcitonin gene related peptide with idealized amphiphilic alpha-helices of different lengths. Biochemistry 27:7600–7607
30. Zull JE, Lev NB 1980 A theoretical study of the structure of parathyroid hormone. Proc Natl Acad Sci USA 77:3791–3795
31. Cohen FE, Strewler GJ, Bradley MS, Carlquist M, Nilsson M, Ericsson M, Ciardelli TL, Nissenson RA 1991 Analogues of parathyroid hormone modified at postions 3 and 6: effects on receptor binding and activation of adenylyl cyclase in kidney and bone. J Biol Chem 266:1997–2004
32. Fiskin AM, Cohn DV, Peterson GS 1977 A model for the structure of bovine parathormone derived by dark field electron microscopy. J Biol Chem 252:8261–8268
33. Chou PY, Fasman GD 1978 Emperical predictions of protein conformation. Annu Rev Biochem 47:251–276
34. Kaiser ET 1987 Design of amphiphilic peptides. In: Oxender DL, Fox CF (eds) Protein Engineering. Liss, New York, vol 1:193–199
35. Reppe S, Gabrielsen OS, Olstad OK, Morrison N, Sæther O, Blingsmos OR, Gautvik VT, Gordeladze J, Haflan AK, Voelkel EF, Øyen TB, Tashjian Jr AH, Gautvik KM 1991 Characterization of a K26Q site-directed mutant of human parathyroid hormone expressed in yeast. J Biol Chem 266:14198–14201
36. Abou-Samra A-B, Freeman M, Juppner H, Uneno S, Segre GV 1990 Characterization of fully active biotinylated parathyroid hormone analogs. J Biol Chem 265:58–62
37. Nussbaum SR, Beaudette NV, Fasman GD, Potts Jr JT, Rosenblatt M 1985 Design of analogues of parathyroid hormone: a conformational approach. J Protein Chem 4:391–406
38. Fujimori A, Cheng S-L, Avioli LV, Civitelli R 1992 Structure-function relationships of parathyroid hormone; activation of phospholipase-C, protein kinase-A and -C in osteosarcoma cells. Endocrinology 130:29–36
39. Jouishomme H, Whitfield JF, Chakravarthy B, Durkin JP, Gagnon L, Isaacs RJ, MacLean S, Neugebauer W, Willick G, Rixon RH 1992 The protein kinase-C activation domain of the parathyroid hormone. Endocrinology 130:53–59
40. Schlüter K-D, Hellstern H, Wingender E, Mayer H 1989 The central part of parathyroid hormone stimulates thymidine incorporation of chondrocytes. J Biol Chem 264:11087–11092

Binding Domain of Human Parathyroid Hormone Receptor: From Conformation to Function†,‡

Maria Pellegrini,§ Alessandro Bisello,|| Michael Rosenblatt,|| Michael Chorev,|| and Dale F. Mierke*,§

Department of Molecular Pharmacology, Physiology, & Biotechnology, Division of Biology & Medicine, and Department of Chemistry, Brown University, Providence, Rhode Island 02912, and Division of Bone and Mineral Metabolism, Charles A. Dana & Thorndike Laboratories, Department of Medicine, Beth Israel Deaconess Medical Center, Harvard Medical School, 330 Brookline Ave., Boston, Massachusetts, 02215

Received May 27, 1998; Revised Manuscript Received July 23, 1998

ABSTRACT: A 31 amino acid fragment of the extracellular N-terminus of the human G-protein coupled receptor for parathyroid hormone (PTH1R) has been structurally characterized by NMR and molecular dynamics simulations. The fragment PTH1R[168−198] includes residues 173−189, shown by photoaffinity cross-linking to be a contact domain with position 13 of parathyroid hormone (PTH). The structure of PTH1R[168−198], determined in a micellar solution of dodecylphosphocholine to mimic the membrane environment, consists of three α-helices, separated by a well-defined turn and a flexible region. The topological orientation of PTH1R[168−198] was determined from nitroxide-radical induced relaxation of NMR signals utilizing 5- and 16-doxylstearic acid. The C-terminal helix (residues 190−196), consisting of seven amino acids of the first transmembrane domain, is very hydrophobic and embedded in the lipid core. This helix is preceded by a well-defined turn, forming an approximate 90° bend, placing the other helices (residues 169−176 and 180−189), both of which are amphipathic, on the surface of the micelle. In this orientation, many hydrophilic residues of the receptor, including Glu^{177}, Arg^{179}, Arg^{181}, Glu^{182}, Asp^{185}, and Arg^{186}, are projecting toward the solvent available to form complementary Coulombic interactions with the polar residues of the principal binding domain of the ligand (e.g., Arg^{25}, Lys^{26}, Lys^{27}, Asp^{30}, and His^{32}). Given that the binding domain of PTH adopts an amphipathic α-helix which lies on the membrane, we visualize ligand binding as a two stage process involving a nonspecific hydrophobic interaction of amphipathic helices with the membrane, followed by two-dimensional diffusion leading to highly specific, ligand−receptor interaction.

Parathyroid hormone (PTH)[1] is the principal regulator of calcium and phosphate ion homeostasis. PTH is active through a G-protein coupled receptor (PTH1R) (*1*, *2*) affecting two intracellular signaling pathways: adenylyl cyclase/cAMP/protein kinase A and inositol triphosphate/cytosolic calcium/protein kinase C. PTH1R belongs to a subfamily of G-protein coupled receptors, presumed to exhibit the characteristic seven membrane-spanning helices as in rhodopsin, sharing a long amino-terminal extracellular region, multiple glycosylation sites, and eight conserved extracellular cysteine residues (*3*). Recent mutational and chimera studies of PTH1R indicate that the extracellular, amino-terminus constitutes one of the sites for ligand/receptor interaction (*4*−*6*). Studies of the ligand have shown that the N-terminal 1−34 fragment of the hormone, PTH[1−34], is equipotent to native PTH and that residues 25−34 constitute the principal binding domain (*7*, *8*).

Recent photoaffinity cross-linking experiments have directly identified a contact between position 13 of PTH and a domain comprising residues 173−189 of the N-terminus of PTH1R, adjacent to the putative first transmembrane helix (TM1) (*9*). To obtain structural insight into the interaction between the receptor and ligand, we have undertaken the investigation of the conformational propensities of both. The NMR-derived structures of human PTH(1−34) in a membrane mimetic show a well-defined amphipathic α-helix for the C-terminal binding domain (*10*). Molecular modeling of human PTH1R, based on the rhodopsin/bacteriorhodopsin structure (*11*, *12*) and homology analysis (*13*), suggested that the contact domain, PTH1R[173−189], adopts an amphipathic α-helix (unpublished data). On the basis of this, one may postulate complementary helix−helix interactions as one

† This work was supported, in part, by Grants R29-GM54082 (to D.F.M.) and R01-DK47940 (to M.R.) from the National Institutes of Health.

‡ The structure coordinates have been deposited in the Brookhaven Protein Data Bank (filename 1BL1).

* To whom correspondence should be addressed. Phone: (401) 863-2139. Fax: (401) 863-1595. E-mail: Dale_Mierke@Brown.edu.

§ Brown University.

|| Harvard Medical School.

[1] Abbreviations: doxyl, 4,4-dimethyl-3-oxazolidinyloxy; DG, distance geometry; G-Protein, guanine nucleotide-binding regulatory protein; MD, molecular dynamics; NMR, nuclear magnetic resonance; NOE, nuclear Overhauser enhancements; PTH, human parathyroid hormone; PTHrP, parathyroid hormone-related protein; PTH1R, parathyroid hormone receptor 1; ROESY, rotational-Overhauser enhancement spectroscopy; DPC, dodecylphosphocholine; TM, transmembrane; TOCSY, total-correlation spectroscopy; DQF-COSY, double quantum filtered correlation spectroscopy, NOESY, nuclear Overhauser enhancement spectroscopy.

S0006-2960(98)01265-3 CCC: $15.00
Published on Web 08/22/1998

of the elements in ligand−receptor recognition and binding. To test this hypothesis, we have examined the conformational characteristics of PTH1R[168−198] in the presence of dodecylphosphocholine micelles by NMR and distance geometry (DG) calculations. We subsequently incorporated free radical bearing fatty acids in the micelles to explore (by NMR) the orientation of the peptide relative to the membrane mimetic. Extensive molecular dynamics (MD) calculations, utilizing a decane/water simulation cell (*14*), have been carried out to obtain the final, refined structures and to describe the partition behavior of the molecule between the two solvents. From the inspection of the high-resolution structure of PTH1R[168−198], the specific amino acids of the receptor in this contact domain available for interaction with the ligand have been identified.

EXPERIMENTAL PROCEDURES

Peptide Synthesis. The peptide, Ac−SEAVKFLTNETR-EREVFDRLGMIYTVGYSVC−NH_2, PTH1R[168−198], was synthesized by solid-phase methodology with an Applied Biosystems 430A peptide synthesizer as described (*15*). The purity was established by analytical high-performance liquid chromatography and the structural integrity by amino acid analysis and electron-spray mass spectrometry.

NMR Methods. PTH1R[168−198] was examined in aqueous solution (ca. 2.4 mM, 9:1 $H_2O/^2H_2O$, pH 4.5 not corrected), in the presence of 150 mM dodecylphosphocholine-d_{38} (DPC). All of the experiments were recorded on a Varian Unity 500 spectrometer at temperatures varying between 298 and 318 K. Data processing utilized Varian software (VNMR) or *Felix* (Biosym/MSI, San Diego). Chemical shifts were referenced to the signal of tetramethylsilane (0.0 ppm).

The amino acid spin systems were identified from DQF−COSY (*16*) and TOCSY (*17*, *18*) spectra. NOESY (*19*, *20*) experiments with mixing times of 125−350 ms were employed for the sequential assignment. The TOCSY utilized a MLEV-17 sequence to realize mixing times of 35−70 ms with a spin-lock field of 10 000 Hz. Suppression of the solvent signal was achieved by continuous wave presaturation at low power during the relaxation delay (1.5−2 s). The NOESY experiments utilized additional presaturation during the mixing time, or alternatively, coupled a "jump and return" observation pulse (*21*) with 0.4 s of presaturation. The typical spectral width was 5000 Hz in both dimensions, with 4096 data points in t_2 and 320−512 data points in t_1 and with 32−128 scans at each increment. Forward linear prediction to 1024 points was applied to the incremented dimension; both dimensions were multiplied by Gaussian or shifted squared sine bell apodization functions, prior to Fourier transformation.

Radical-Induced Relaxation. The 5- and 16-doxylstearic acid were solubilized in methanol-d_4 to a final concentration of 53 mM. Aliquots of this solution were added to the solution of peptide and DPC to obtain 0.25−0.94 mM concentrations of the spin-label. The titrations with 5- and 16-doxylstearic acid were carried out separately on two equivalent peptide solutions. TOCSY experiments (mixing time 35 ms) were recorded under identical conditions before and after the addition of the doxylstearic acid. The intensities of cross-peaks involving both backbone (H^N-H^α) and side chain protons ($H^\alpha-H^\beta$, $H^\gamma-H^\delta$) were compared.

Distance Geometry. NOESY spectra acquired at 298, 308, and 318 K with a mixing time of 150 ms (with 10% randomization) were utilized to measure cross-peaks volumes. The volumes were converted to distances using the two-spin approximation. The resolved cross-peak between two protons within the α-helical domain of the peptide was utilized as a reference (Phe^{184} H^N-Asp^{185} H^N, 2.8 Å) (*22*, *23*). Addition and subtraction of 10% to the calculated distances yielded upper and lower bounds. Pseudoatom corrections were applied to methyl groups and methylene protons with coincident chemical shifts (*22*); the floating chirality approach (*24*) was utilized for nonstereospecifically assigned, resolved methylene protons. A home-written program was utilized to calculate an ensemble of structures fulfilling holonomic (constitutional) and experimental (proton−proton distances) restraints. The two-step procedure utilizes the random metrization algorithm (*25*) followed by optimization via conjugate gradients (*26*), and by distance driven dynamics (DDD) (*27*, *28*). The procedure is repeated first in four dimensions, for optimal sampling of the conformational space, and then in three dimensions. The final DDD on the 98 calculated structures was carried out at 500 K for 200 ps, followed by slow cooling to 0 K.

Molecular Dynamics. MD simulations were performed with GROMACS, version 1.6 (*29*). Interactive modeling utilized *Insight II* (Biosym/MSI, San Diego). To produce a solvent system consistent with the experimental conditions (water and DPC micelles) and acceptable computation times on standard workstations, a two-phase box of water and decane was implemented. A detailed description of the decane/water interface has appeared (*14*). All atoms were treated explicitly except for the CH_n atoms of the decane molecules which were treated as united atoms. For the dihedral angles $CH_2CH_2CH_2CH_2$ and $CH_2CH_2CH_2CH_3$ of decane, the Ryckaert-Bellemans potential was used (*14*, *30*). The single-point-charge (SPC) model was adopted for water (*31*, *32*). Initially a layer of decane was created, containing 100 molecules in the all-trans configuration and with parallel head-to-tail axes. This box underwent energy minimization for 200 steps (steepest descent) and 100 ps of molecular dynamics at 300 K, with a time constant of 2 fs. A twin-range cutoff for nonbonded forces of 0.8/1.0 nm was used; the pair list and forces for the range 0.8−1.0 nm were updated every 10 steps. A second layer of water was added utilizing a cubic box of 216 equilibrated SPC water molecules. The water molecules were allowed to keep a minimum distance of 0.23 nm from the atoms of the decane molecules. The two-phase cell, of dimensions 4.7 × 4.7 × 4.7 nm, underwent energy minimization and MD utilizing the conditions described above. The final cell was utilized to soak PTH1R[168−198].

One of the low-violation DG structures was used as the starting structure for the MD simulation. The molecule was placed in the (periodic) two-phase box of H_2O/decane, containing 992 water and 123 decane molecules in a volume of 101.6 nm^3. The charges of ionizable groups correspond to the pH of the NMR solution; no counterions were included. The system was energy minimized for 100 steps (steepest descent). In the following 10 ps of MD at 300 K (*33*), the peptide was restrained to its original position with

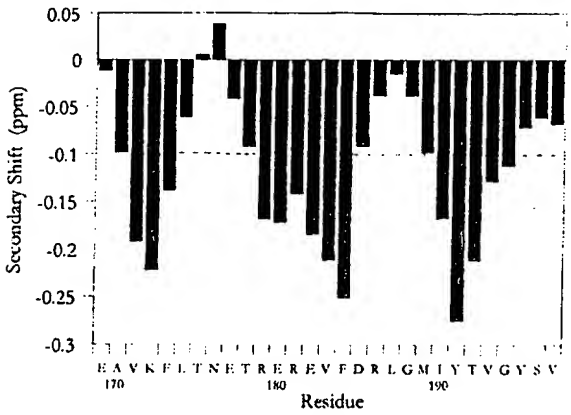

FIGURE 1: The secondary shifts of the α-protons of PTH1R[168−198] in aqueous solution (2.4 mM, pH 4.5) in the presence of DPC (150 mM) micelles.

a force constant of 1000 kJ mol^{-1} nm^{-1}. Experimental distance restraints were then introduced with a force constant of 10 000 kJ mol^{-1} nm^{-1} for the 400 ps of the simulation. Structures were sampled every 0.5 ps. One iteration took approximately 0.52 s on a SGI O2 (R5000, 200 MHz). The resulting trajectories were examined with analysis programs in the GROMACS package and home-written Fortran programs.

RESULTS

PTH1R[168−198] contains the 17 amino acid contact domain (residues 173−189) previously identified to cross-link to position 13 of PTH[1−34] (*9*). This contact domain was extended by nine amino acids at the C-terminus to include the hydrophobic residues postulated to be the beginning of TM1. These residues were included to anchor and orient the receptor fragment into the micelle. The dodecylphosphocholine micelles, utilized to mimic the membrane environment in the NMR studies, were also required for solubilization. In benign aqueous solution, the peptide formed a semisolid gel in approximately 20 min, which could not be resolubilized by variation of pH or ionic strength. Furthermore the DPC micelles provide a charged, zwitterionic interface and a hydrophobic core, properties of the biological membrane in which the receptor is located. Additionally, the micelle undergoes rapid reorientation in solution allowing for high-resolution NMR studies. The concentration of the DPC was adjusted to ensure more than one micelle per each peptide molecule (*34*, *35*).

Secondary Structure. The secondary shifts for H^{α} were calculated by subtracting the chemical shifts for unstructured peptides (*22*) from the experimentally measured chemical shifts and averaging the values over succeeding triplets of amino acids (*35*). The negative values observed for Ala^{170}−Leu^{174}, Thr^{178}−Asp^{185}, and Met^{189}−Tyr^{195} (Figure 1) are consistent with α-helical structure (*36*). At two positions along the sequence (in addition to the peptide termini), the H^{α} chemical shifts adopt random-coil values, indicating interruptions in the helical structure around residues Thr^{175} and Leu^{187}. The relevant nonsequential NOEs are reported in Figure 2. A series of correlations of type H^{N}_{i} to H^{N}_{i+1} or H^{N}_{i+2} and H^{α}_{i} to H^{N}_{i+3} or H^{N}_{i+4} confirms the presence of the three α-helical regions. In addition, strong NOEs of type H^{α}_{i} to H^{N}_{i+2} between Thr^{175}−Glu^{177} and Arg^{186}−Gly^{188} suggest the presence of turns.

A total of 83 structures were obtained from the DG calculations, with small penalty functions and no NOE violation. The structures converge to fairly regular α-helical segments encompassing residues 169−176, 181−189, and 192−195. The dihedral angle order parameters for ϕ and ψ (data not shown) indicate a high degree of order in the regions 169−176 and 180−195. The high disorder at Thr^{178} prevents the assessment of a preferred orientation of the N-terminal helix relative to the rest of the molecule. This disorder may be caused by the lack of experimental restraints, resulting from spectral overlap, rather than conformational disorder or flexibility. From Arg^{179} to the C-terminus the DG structures can be described as two consecutive helices forming an angle of ca. 90° between their axes. Interestingly, both the extracellular helix and the turn separating it from TM1 were correctly predicted by homology modeling of PTH1R (unpublished data). The average pairwise root-mean-square deviation (RMSD) of the backbone atoms of the entire peptide over the 83 structures is 5.5 Å. The ordered regions are characterized by an RMSD of 0.78 Å for residues 169−176, 1.46 Å for the second helix (residues 180−189), and 1.06 Å for the residues of the putative TM1 (190−196). Thirty structures from the DG calculations are represented in Figure 3. The structures have been superimposed in the C-terminal region to illustrate the well-defined second and third helical domains as well as the turn between these domains. As discussed above, the N-terminal helix assumes a range of different orientations relative to the rest of the molecule.

Topological Orientation. The topological orientation of the peptide relative to the DPC micelle was determined by titration with 5- and 16-doxylstearic acid, carrying a nitroxide radical at positions 5 and 16, respectively. The doxylstearic acid readily incorporates into DPC micelles, placing the nitroxide radical at the same level as the phosphate head-groups (5-doxyl) or slightly off-center from the core of the micelle (16-doxyl) (*38*). Upon addition of the doxylstearic acid to the peptide solution, NMR signals in close proximity to the radical are significantly broadened (a small background broadening of all resonances is usually observed) (*38*−*40*).

In the presence of 5-doxylstearic acid, most of the residues show a reduced intensity, indicating that a majority of the amino acids are proximal to the charged membrane surface (Figure 4A). In particular, the N-terminal helix displays a periodicity that agrees with an α-helix lying on the surface (i.e., the residues projecting into the solution are distal from the nitroxide radical). The effect on the other two helices is less specific, consistent with an orientation in which the residues are partially embedded in the micelle. The titration with 16-doxylstearic acid, which places the nitroxide near the center of the micelle, is expected to significantly affect only those residues in the hydrophobic core. Indeed, a reduction of intensity greater than 25% was observed for residues from Thr^{192} to the C-terminus. Residues 183−191 were moderately affected, while the N-terminal residues displayed almost no variation (see Figure 4B).

Conformation and Partition Behavior from MD. The starting structure, generated from the DG calculations, was placed in the biphasic water/decane cell with an orientation

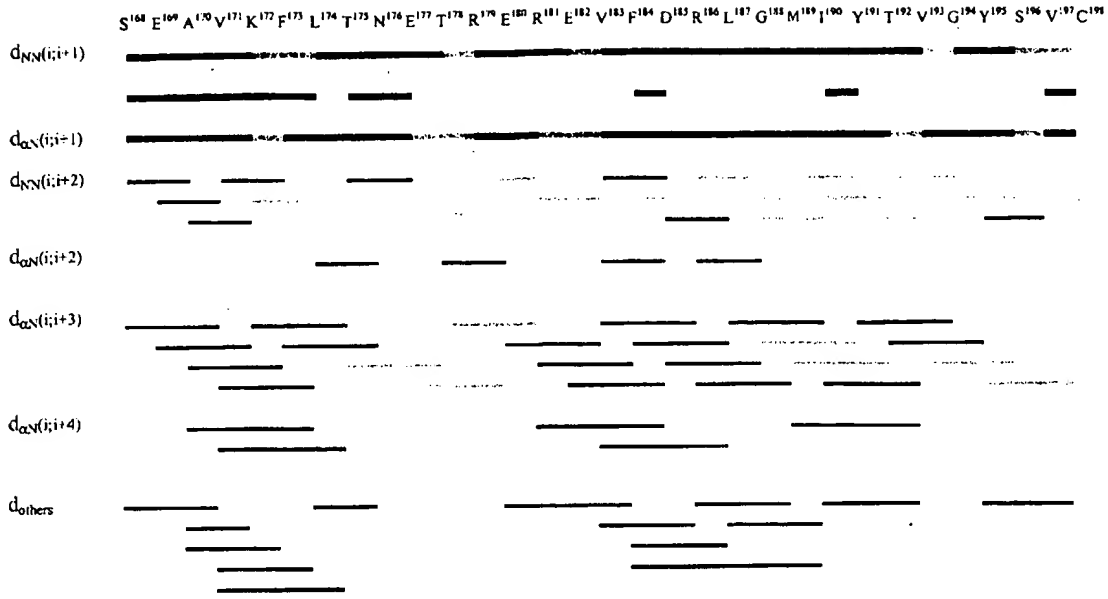

FIGURE 2: Relevant NOEs detected from NOESY spectra at 298, 308, and 318 K and utilized in the structure calculations. A shaded bar indicates a cross-peak not unambiguously identified due to resonance overlap.

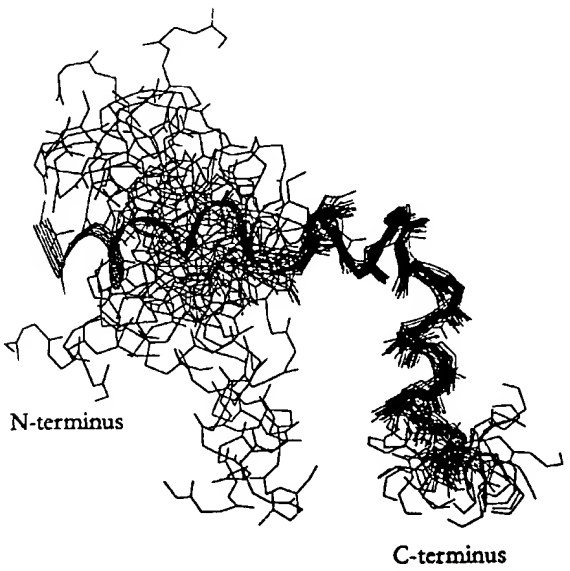

FIGURE 3: Backbone representation of 30 structures, with the backbone atoms of residues 180−198 superimposed, obtained from DG calculations.

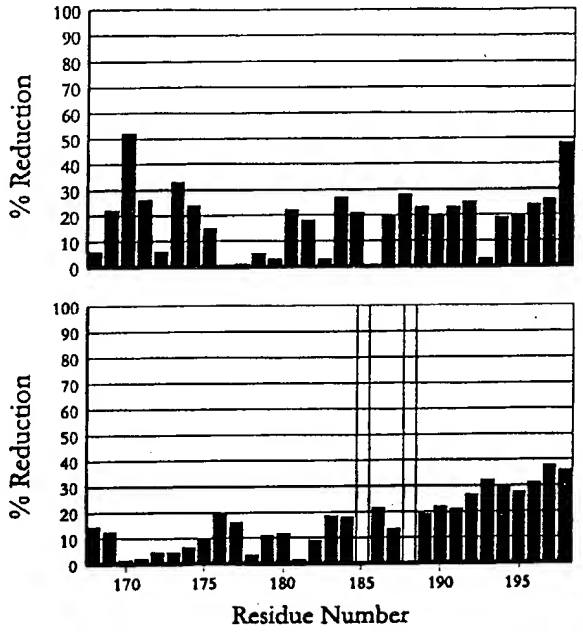

FIGURE 4: Histograms representing the reduction in cross-peak intensity for single residues (measured from TOCSY spectra) upon addition of 5-doxylstearic acid (top) or 16-doxylstearic acid (bottom). Empty bars indicate residues for which data could not be obtained.

based on the results of the NMR experiments in the presence of nitroxide radicals. The C-terminal helix (corresponding to the extracellular end of TM1), which was determined to be in the hydrophobic core of the micelle, was embedded in the decane phase with the helix axis perpendicular to the interface. This placed the other two helices at the interface, largely exposed to the water phase, in agreement with the results of the nitroxide-radical experiments. This orientation was maintained for the entire simulation (400 ps). The secondary structure and the tertiary arrangement of the three helices did not show significant changes, and no violation of the experimental distance restraints was observed (Figure 5). A second simulation was carried out to explore the most favorable partitioning of the peptide between the two media.

For this simulation, the peptide was placed entirely in the decane phase with the N-terminal helix directed away from the interface. During the first 70 ps of the simulation, the peptide translated and reoriented relative to the plane of the interface so that the N-terminal and middle helices reached the water phase, finally adopting the same orientation as obtained from the first simulation. No rearrangement of the secondary or tertiary structure was observed during this major redistribution of the molecule between the two solvents. The average backbone dihedral angles resulting from the MD simulation are reported in Table 1.

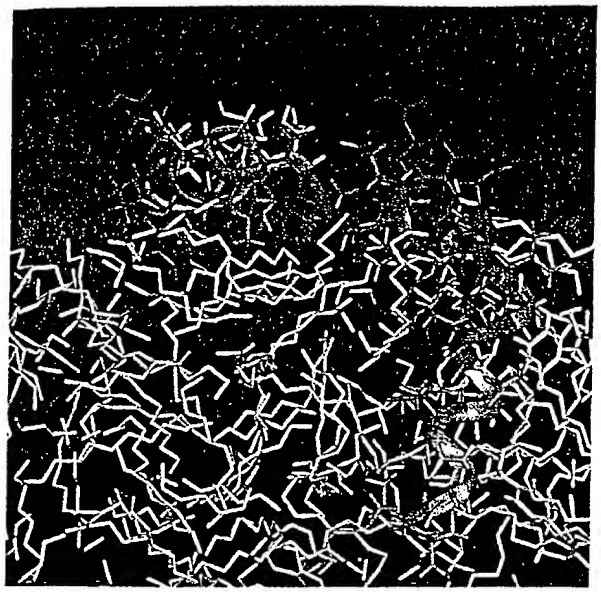

FIGURE 5: A structure of PTH1R[168−198] from the MD calculation in a water/decane simulation cell. The peptide ribbon is colored according to hydrophobicity (blue = polar, red = hydrophobic); the decane molecules are depicted in yellow and the water molecules are not displayed for clarity. The residues belonging to TM1 are to the right of the cell, embedded in the decane phase.

Table 1: Average Dihedral Angles and Standard Deviation from the Last 50 ps of Decane/Water MD Simulation

residue	ϕ	ψ
Glu^{169}	−46.7 ± 6	−37.2 ± 5
Ala^{170}	−65.7 ± 8	−45.6 ± 7
Val^{171}	−62.3 ± 5	−35.1 ± 6
Lys^{172}	−60.2 ± 6	−37.6 ± 11
Phe^{173}	−78.5 ± 11	−38.5 ± 6
Leu^{174}	−56.5 ± 9	−49.2 ± 6
Thr^{175}	−67.7 ± 9	−23.1 ± 11
Asn^{176}	−60.3 ± 11	−41.4 ± 9
Glu^{177}	−147.6 ± 11	82.5 ± 8
Thr^{178}	−76.0 ± 9	59.5 ± 19
Arg^{179}	−99.4 ± 19	−14.0 ± 10
Glu^{180}	−62.3 ± 11	−63.9 ± 11
Arg^{181}	−62.1 ± 8	−33.1 ± 9
Glu^{182}	−61.9 ± 11	−39.9 ± 12
Val^{183}	−90.8 ± 11	−20.1 ± 7
Phe^{184}	−92.4 ± 8	12.9 ± 10
Asp^{185}	−103.3 ± 9	−26.3 ± 9
Arg^{186}	−77.7 ± 7	30.7 ± 9
Leu^{187}	−43.1 ± 8	−30.5 ± 5
Gly^{188}	−65.0 ± 8	−11.9 ± 9
Met^{189}	−111.0 ± 7	−8.8 ± 9
Ile^{190}	−90.8 ± 7	−69.1 ± 6
Tyr^{191}	−55.0 ± 6	−35.2 ± 6
Thr^{192}	−50.7 ± 10	−59.3 ± 5
Val^{193}	−59.6 ± 6	−43.2 ± 6
Gly^{194}	−52.6 ± 7	−40.5 ± 13
Tyr^{196}	−70.9 ± 12	−57.3 ± 9
Ser^{197}	−77.1 ± 12	15.1 ± 28
Val^{198}	−82.9 ± 22	−27.8 ± 26

DISCUSSION

The investigation of PTH1R[168−198] was undertaken to structurally characterize a region of the human PTH1 receptor previously implicated in ligand binding (*9*). This represents an experimental approach to obtaining structural insight into membrane-embedded receptors, which as a whole, cannot generally be examined by conventional methods (X-ray crystallography, NMR spectroscopy). The choice of experimental conditions is crucial; the receptor fragment examined here, containing approximately seven residues of TM1, quickly forms a semisolid gel in water. The aqueous solution of DPC micelles provides an NMR-compatible solvent system that mimics the interface between the membrane and extracellular milieu. Indeed, all experimental results (including line broadening in the NMR spectra, TOCSY experiments with correlation behavior typical of very large molecules, and titrations with free radicals) indicate that the peptide is tightly associated with the micelle and adopts a topological orientation fully consistent with that expected for this fragment in native PTH1R.

The seven amino acids corresponding to TM1 adopt an α-helix which embeds into the hydrophobic core of the micelle. The remainder of the receptor fragment, amphipathic in nature, lies at the interface on the micelle surface with the hydrophobic face directed toward the micelle. In particular, the NMR resonances of residues Ala^{170}, Val^{171}, Phe^{173}, and Leu^{174}, on the hydrophobic face of the N-terminal helix, are significantly broadened by the addition of 5-doxylstearic acid and therefore lie at the micelle surface. In contrast, Glu^{169}, Lys^{172}, and Asn^{176}, making up the hydrophilic face of the N-terminal helix, are unaffected and likely exposed to the solvent.

The H_2O/decane box used for the MD simulations reproduces the biphase character of the aqueous micellular solution. The decane molecules mimic the hydrophobic phase created by the alkylic chains of the DPC molecules. In this simulation system, the correct description of the charged interface, created by the phosphate and choline groups of the DPC, is sacrificed for simplicity and computational speed, which in turn allows for extended simulations starting from different orientations. The goal of the simulations is further refinement of the receptor and verification of the energetic stability of the DG-generated structures in an environment similar to that used for the NMR experiments. Additionally, the simulations provided further evidence for the preferred partitioning of the molecule between the hydrophobic and hydrophilic phases. Despite the fact that no constraint on the location of the peptide within the two-phase box was applied, the TM1 helix was always found embedded in the decane phase, approximately perpendicular to the interface. The remaining peptide chain prefers to occupy a position at the interface, allowing for optimal interactions of the two amphipathic helices with the solvents. This topological arrangement is in complete accord with the experimental results and fully consistent with that expected for this region in the intact receptor.

While the placement and relative arrangement of the seven TM helices in G-protein coupled receptors is relatively well understood from the studies of rhodopsin and bacteriorhodopsin (*11*) and other membrane embedded proteins (chiefly the bacterial reaction center), little is known about the structure of the intra- and extracellular termini and loops. The determination of the structural elements of the loops and termini would afford important insight into the biomolecular interactions of the receptor with the G-protein (intracellular domain) (*40*−*42*) and with the hormone-ligand (extracellular domain) (*43*, *44*). These studies would reveal the determinants which confer the specificity of ligand-

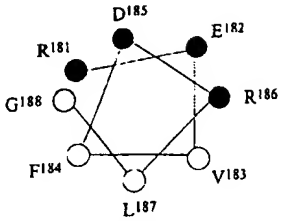

PTH1R(181-188)

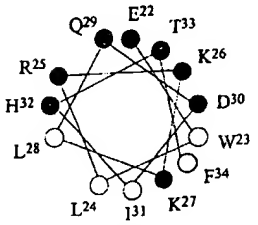

PTH(22-34)

FIGURE 6: Helical wheel diagrams depicting the amphipathic α-helical regions of PTH1R[168−198] (top) and PTH (bottom) which have been shown to associate with the micelle surface. The hydrophilic residues are filled, the hydrophobic residues are open.

recognition and signal transduction. In this study, the conformational features and topological orientation of an extracellular fragment of the PTH1R, associated with ligand binding, are reported.

The NMR-derived structure of PTH(1−34), a fully potent fragment of PTH, in the presence of DPC micelles was recently described (*10*). The results indicate that the C-terminus, including the binding domain [residues 25−34 (*8*)], adopts an amphipathic α-helix, which lies on the surface of the lipid. The current finding that the contact domain of PTH1R, residues Phe^{173}−Met^{189}, also folds into an amphipathic α-helix and lies on the lipid surface suggests a possible interaction between ligand and receptor. We propose that the initial binding event involves the amphipathic α-helices of the ligand (consisting of residues 19−33 of PTH) (*10*, *45*) and receptor (residues 181−189 and possibly, the N-terminal helix, residues 169−176), all of which have been experimentally verified to readily associate with the membrane surface. Helical wheel diagrams of these regions of PTH and receptor fragment are depicted in Figure 6. A theory that the recognition of peptide hormones by membrane bound receptors is preceded by nonspecific preadsorption on the target cell membrane has been described (*46*, *47*). The theory proposes that the hydrophobic adsorption is followed by a random, two-dimensional diffusion leading to lateral collisions of the folded structure (membrane-induced structure) of the peptide hormone with the receptor. If this is the case, the amino acids exposed to the solution, available for helix−helix interaction, would be crucial for binding. The hydrophilic face of the receptor helix includes Glu^{177}, Arg^{179}, Arg^{181}, Glu^{182}, Asp^{185}, and Arg^{186}. The charges of these amino acids readily avail themselves to Columbic interactions with the complementarily charged residues of the amphipathic helix of the ligand, including Arg^{25}, Lys^{26}, Lys^{27}, and Asp^{30}. These helix−helix interactions provide the affinity and specificity associated with ligand binding. To test this model, the importance of each of these residues, individually and pairwise, for ligand binding must be examined. It is important to note that the receptor fragment examined here probably constitutes only one domain of the ligand binding pocket and the role of the remainder of the N-terminus, as well as the extracellular loops, in the formation of the ligand−receptor complex will have to be determined.

REFERENCES

1. Suva, L. J., Winslow, G. A., Wettenhall, R. E. H., Hammond, R. G. G., Moseley, J. M., Diefenback-Jagger, H., Rodda, C. P., Kemp, B. E., Rodriguez, H., Chen, E. Y., Hundson, P. J., and Martin, T. J. (1987) *Science 237*, 893−896.
2. Jüppner, H., Abou-Samra, A. B., Freeman, M. W., Kong, X. F., Schipani, F., Richards, J., Kolakowski, L. F. J., Hock, J., Potts, J. T., Jr, and Kronenberg, H. M. (1991) *Science 254*, 1024−1026.
3. Segre, g. V., and Goldring, S. R. (1993) *Trends Endocrinol. Metab. 4*, 309−314.
4. Bergwitz, C., Gardella, T. J., Flannery, M. R., Potts, J. T. j., Kronenberg, H. M., Goldring, S. R., and Juppner, H. (1996) *J. Biol. Chem. 271*, 26469−26472.
5. Lee, C., Gardella, T. J., Abou-Samra, A. B., Nussbaum, S. R., Segre, G. V., Potts, J. T., Jr., Kronenberg, H. M., and Jüppner, H. (1994) *Endocrinology 135*, 1488−1495.
6. Urena, P., Abou Samra, A. B., Jüppner, H., Kong, X. F., Lee, K., Bringhurst, F. R., and Segre, G. V. (1994) *Ann. Endocrinol. (Paris) 55* (54O), 133−141.
7. Rosenblatt, M., Callahan, E. N., Mahaffey, J. E., Pont, A., and Potts, J. T., Jr. (1977) *J. Biol. Chem. 252*, 5847−5851.
8. Nussbaum, S. R., Rosenblatt, M., and Potts, J. T., Jr. (1980) *J. Biol. Chem. 255*, 10183−10187.
9. Zhou, A. T., Bessalle, R., Bisello, A., Nakamoto, C., Rosenblatt, M., Suva, L. J., and Chorev, M. (1997) *Proc. Natl. Acad. Sci. U.S.A. 94*, 3644−3649.
10. Pellegrini, M., Royo, M., Rosenblatt, M., Chorev, M., and Mierke, D. F. (1998) *J. Biol. Chem. 273*, 10420−10427.
11. Pebay Peyroula, E., Rummel, G., Rosenbusch, J. P., and Landau, E. M. (1997) *Science 277*, 1676−1681.
12. Schertler, G. F., Villa, C., and Henderson, R. (1993) *Nature 362*, 770−772.
13. Altshul, S. F., Gish, W., Miller, W., Myers, E. W., and Lipman, D. J. (1990) *J. Mol. Biol. 215*, 403−410.
14. van Buuren, A. R., Marrink, S., and Berendsen, H. J. C. (1993) *J. Phys. Chem. 97*, 9206−9216.
15. Nakamoto, C., Behar, V., Chin, K. R., Adams, A. E., Suva, L. J., Rosenblatt, M., and Chorev, M. (1995) *Biochemistry 34*, 10546−10552.
16. Rance, M., Sørensen, O. W., Bodenhausen, G., Wagner, G., Ernst, R. R., and Wüthrich, K. (1983) *Biochem. Biophys. Res. Commun. 117*, 458−479.
17. Braunschweiler, L., and Ernst, R. R. (1983) *J. Magn. Reson. 53*, 521−528.
18. Bax, A., and Davis, D. G. (1985) *J. Magn. Reson. 65*, 355−360.
19. Jeener, J., Meier, B. H., Bachmann, P., and Ernst, R. R. (1979) *J. Chem. Phys. 71*, 4546−4553.
20. Macura, S., Huang, Y., Suter, D., and Ernst, R. R. (1981) *J. Magn. Reson. 43*, 259−281.
21. Plateau, P., and Gueron, M. (1982) *J. Am. Chem. Soc. 104*, 7310−7311.
22. Wüthrich, K. (1986) *NMR of Proteins and Nucleic acids*, Wiley, New York.
23. Cavanagh, J., Fairbrother, W. J., Palmer, A. G., and Skelton, N. J. (1996) *Protein NMR Spectroscopy, Principle and Practice*, Academic Press, New York.
24. Weber, P. L., Morrison, R., and Hare, D. (1988) *J. Mol. Biol. 204*, 483−487.
25. Havel, T. F. (1991) *Prog. Biophys. Mol. Biol. 56*, 43−78.
26. Kaptein, R., Boelens, R., Scheek, R. M., and van Gunsteren, W. F. (1988) *Biochemistry 27*, 5389−5395.
27. Mierke, D. F., Geyer, A., and Kessler, H. (1994) *Int. J. Pept. Protein Res. 44*, 325−331.

28. Jahnke, W., Mierke, D. F., Beress, L., and Kessler. (1994) *J. Mol. Biol. 240*, 445−458.
29. van der Spoel, D., van Buuren, A. R., Apol, E., Meulenhoff, P. J., Tieleman, D. p., Sijbers, A. L. T. M., van Drunen, R., and Berendsen, H. J. C. (1996) *Gromacs User Manual*, University of Groningen.
30. Ryckaert, J. P., and Bellemans, A. (1978) *Faraday Discuss. Chem. Soc. 66*, 95.
31. Berendsen, H. J. C., Postma, J. P. M., van Gunsteren, W. F., and Hermans, J. (1981) *Intermolecular forces*, pp 331−342, D. Reidel Publishing Co., Dodrecht.
32. Miyamoto, S., and Kollman, P. A. (1992) *J. Comput. Chem. 13*, 952−962.
33. Berendsen, H. J. C., Postma, J. P. M., DiNola, A., and Haak, J. R. (1984) *J. Chem. Phys. 81*, 3684−3690.
34. McDonnel, P. A., and Opella, S. J. (1993) *J. Magn. Reson. B 102*, 120−125.
35. Kallick, D. A., Tesmer, M. R., Watts, C. R., and Li, C. (1995) *J. Magn. Reson. B 109*, 60−65.
36. Pastore, A., and Saudek, V. (1990) *J. Magn. Reson. 90*, 165−176.
37. Wishart, D. S., Sykes, B. D., and Richards, F. M. (1992) *Biochemistry 31*, 1647−1651.
38. Brown, L. R., Bösch, C., and Wüthrich, K. (1981) *Biochim. Biophys. Acta 642*, 296−312.
39. van de Ven, F. J. M., van Os, J. W. M., Aelen, J. M. A., Wymenga, S. S., Remerowsky, M. L., Konings, R. N. H., and Hilbers, C. W. (1993) *Biochemistry 32*, 8322−8328.
40. Pellegrini, M., Royo, M., Chorev, M., and Mierke, D. F. (1996) *J. Pept. Sci. 40*, 653−666.
41. Mierke, D. F., Royo, M., Pellegrini, M., Sun, H., and Chorev, M. (1996) *J. Am. Chem. Soc. 118*, 8998−9004.
42. Yeagle, P. L., Alderfer, J. L., Salloum, A. C., Ali, L., and Albert, A. D. (1997) *Biochemistry 36*, 3864−3869.
43. Pervushin, K. V., Yu, V., Popov, A. I., Musina, L. Y., and Arseniev, A. S. (1994) *Eur. J. Biochem. 219*, 571−583.
44. Pashkov, V. S., Balashova, T. A., Zhemaeva, L. V., Sikilnda, N. N., Kutuzov, M. A., Abdulaev, N. G., and Arseniev, A. S. (1996) *FEBS Lett. 381*, 119−122.
45. Mierke, D. F., Maretto, S., Schievano, E., DeLuca, D., Bisello, A., Mammi, S., Rosenblatt, M., Peggion, E., and Chorev, M. (1997) *Biochemistry 36*, 10372−10383.
46. Schwyzer, R. (1986) *Natural Products and Biological Activities*, Tokio Press and Elsevier, Tokio.
47. Moroder, L., Romano, R., Guba, W., Mierke, D. F., Kessler, H., Delporte, C., Winand, J., and Christophe, J. (1993) *Biochemistry 32*, 13551−13559.

BI981265H

Structure and Activities of Constrained Analogues of Human Parathyroid Hormone and Parathyroid Hormone-Related Peptide: Implications for Receptor-Activating Conformations of the Hormones

Jean-René Barbier, Suzanne MacLean, Paul Morley, James F. Whitfield, and Gordon E. Willick*

Institute for Biological Sciences, National Research Council, Ottawa, Ontario, Canada K1A 0R6

Received July 5, 2000; Revised Manuscript Received September 1, 2000

ABSTRACT: Parathyroid hormone (PTH) has a helix−bend−helix structure in solution. Part of the C-terminal helix, residues 21−31, is amphiphilic and forms a critical receptor-binding region. Stabilization of this α-helix by lactam formation between residues spaced *i*, *i* + 4 on the polar face was previously reported to increase adenylyl cyclase-stimulating (AC) activity if between residues 22 and 26 but to diminish it if between residues 26 and 30 [Barbier et al. (1997) *J. Med. Chem. 40*, 1373−1380]. This work reports the effects of other cyclizations on the polar face, differing in ring size or position, on α-helix conformation, as measured by circular dichroism, and on AC-stimulating activity. All analogues cyclized between residues 22 and 26 had at least a 1.5-fold increase in activity, suggesting an α-helical structure between about residues 21 and 26. Cyclization between residues 25 and 29 or residues 26 and 30 diminished activity by 20−30%, despite stabilizing α-helix, suggesting that residues 25−31 bind to the receptor in a helical, but not classical α-helical, conformation. Analogues cyclized between residues 13 and 17 had slightly increased activity. A bicyclic analogue, with lactams between residues 13 and 17 and residues 22 and 26, had about the same activity as that cyclized only between 22 and 26. Parathyroid hormone-related peptide (PTHrP) may bind in a manner similar to the common receptor, but hydrophobic moment calculations suggest that it must bind as a tighter helix in order to optimally present its hydrophobic residues to the receptor. Both PTHrP analogues cyclized between either residues 22 and 26 or residues 26 and 30 had more stable α-helices but reduced AC activities, consistent with this hypothesis.

Parathyroid hormone (PTH)[1] is an endocrine hormone, functioning principally to regulate the extracellular calcium concentration in animals. It can also mimic the various functions of the locally acting parathyroid hormone-related peptide (PTHrP) via their shared PTHR1 (type I PTH/PTHrP) receptor (*1*). This regulation is effected through actions on kidney, intestine, and bone cell receptors. If injected in a pulsatile fashion, PTH has a powerful anabolic effect on bone, an effect that depends on its ability to stimulate adenylyl cyclase in osteoblast receptors (*2*). The N-terminal 28 residues of PTH are required for full AC stimulation (*3*, *4*), with loss of residue 28 resulting in a dramatic loss of activity (*3*, *4*). Full activity of the shorter analogues also requires a C-terminal amide (*4*). The shortest fully osteogenic linear PTH has been identified as hPTH(1−30)NH_2 (*5*), with shorter linear fragments 1−28 and 1−29 being only weakly osteogenic. PTHrP has also been reported to have osteogenic activity (*6*), but its 1−31 fragment, unlike that of PTH, was not active in the ovariectomized rat model of osteoporosis (*7*).

The PTHR1 receptor was identified in opossum kidney in 1991 (*1*), and a closely related one was later isolated from rat osteoblasts (*8*). The major receptor-binding region of PTH was shown to reside in residues 14−34 (*9*), and within this sequence is an α-helical region, residues 17−29, identified in both NMR (*10*−*12*) and CD studies (*4*, *13*). Part of this α-helix, residues 20−34, is amphiphilic, and its hydrophobic face has been postulated to bind to the receptor. In support of this, it has been found that hydrophobic residues in this sequence are especially sensitive to mutation (*14*, *15*), while those on the polar residues can be mutated much more freely without loss of activity. A second short α-helix, between about residues 3 and 9, has been identified in NMR studies of hPTH(1−34) (*10*) and hPTH(1−37) (*12*).

Certain side-chain interactions may be important for stabilizing α-helices, including ion pair formation between residues spaced *i*, *i* + 4 apart (*16*). Natural such ion pairs exist between residues 22 and 26 and residues 26 and 30 in hPTH and between residues 13 and 17 and residues 26 and 30 in hPTHrP (Figure 1). Analogues resulting from the formation of lactams between these residues in hPTH were shown to stabilize an α-helical conformation in the region about the lactam (*17*, *18*) One of these lactam analogues, [Leu^{27}]c(Glu^{22}−Lys^{26})hPTH(1−31)NH_2, has both increased AC-stimulating (*17*) and osteogenic activities (*19*). Furthermore, these same modifications greatly enhance the AC-stimulating activity of hPTH(1−28)NH_2 and make it almost

[1] Abbreviations: CD, circular dichroism; DMF, dimethylformamide; DCM, dichloromethane; GRF, growth hormone-releasing factor; HOBt, hydroxybenzotriazole; PTH, parathyroid hormone; PTHrP, parathyroid hormone-related peptide; ROS, rat osteosarcoma; TBTU, *O*-benzotriazolyl-*N*,*N*,*N*′,*N*′-tetramethyluronium tetrafluoroborate; PyAOP, (7-azabenzotriazol-1-yloxy)tris(pyrrolidino)phosphonium hexafluorophosphate; TFA, trifluoroacetic acid; MALDI-TOF, matrix-assisted laser desorption ionization time-of-flight.

10.1021/bi001527r CCC: $19.00 Published 2000 by the American Chemical Society
Published on Web 11/03/2000

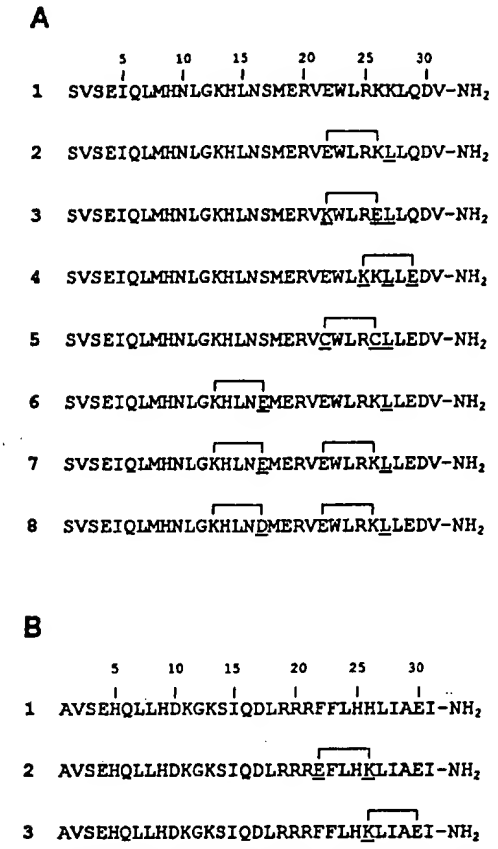

FIGURE 1: Sequences of cyclic analogues described in this paper. Mutated residues are underlined. (A) hPTH analogues: 1, hPTH-(1−31)NH_2; 2, [Leu^{27}]c(Glu^{22}−Lys^{26})hPTH(1−31)NH_2; 3, [Lys^{22},-Glu^{26},Leu^{27}]c(Lys^{22}−Glu^{26})hPTH(1−31)NH_2; 4, [Lys^{25},Glu^{29},-Leu^{27}]c(Lys^{25}−Glu^{29})hPTH(1−31)NH_2; 5, [Cys^{22},Cys^{26},Leu^{27}]c-(Cys^{22}−Cys^{26})hPTH(1−31)NH_2; 6, [Glu^{17},Leu^{27}]c(Lys^{13}−Glu^{17})-hPTH(1−31)NH_2; 7, [Glu^{17},Leu^{27}]c(Lys^{13}−Glu^{17},Glu^{22}−Lys^{26})-hPTH(1−31)NH_2; 8, [Asp^{17},Leu^{27}]c(Lys^{13}−Asp^{17},Glu^{22}−Lys^{26})-hPTH(1−31)NH_2. (B) hPTHrP analogues: 1, hPTHrP(1−31)NH_2; 2, [Glu^{22},Lys^{26}]c(Glu^{22}−Lys^{26})hPTHrP(1−31)NH_2; 3, [Lys^{26}]c-(Lys^{26}−Glu^{30})hPTHrP(1−31)NH_2.

fully osteogenic in the ovariectomized rat model (*20*). We posed the question as to whether all lactams formed between residues on the polar face retain at least major activity, consistent with a postulated mode of receptor binding wherein the region between residues 20 and 31 binds as an α-helix. Aside from those involving natural sequences, such lactams require sequence mutations that must also be analyzed to separate effects arising from those of the linear mutations alone and effects due to conformational restraint imposed by the lactam. The evidence presented here suggests only part of the 21−31 region of hPTH(1−31)NH_2 binds as a classical α-helix, the rest likely binding as some type of distorted helix.

MATERIALS AND METHODS

Chemicals. *N*-α-Fmoc-(*S*)-*p*-methoxytrityl-L-cysteine [Fmoc-Cys(Mmt)] was obtained from NovaBiochem, and other Fmoc-amino acids were from NovaBiochem or Peptides International.

Analogues of hPTH(1−31)NH_2 or hPTHrP(1−31)NH_2 (Figure 1) were synthesized on a MilliGen 9050 continuous-flow peptide synthesizer, with TentaGel S RAM (Rapp Polymere, Tübingen, Germany) as the support and Fmoc chemistry (*21*), as previously described (*17*). Lactams involving residue pairs in the sequence region 22−31 were formed after residue 18 had been added. The lactam between residues 13 and 17 was synthesized after completion of the entire sequence. They were formed as described previously but with PyAOP/HOBt as the activator. Peptides were cleaved from the support with either TFA/phenol/water/thioanisole/ethanedithiol (18.2/1.125/1.125/1.125/0.56 v/v/v/v/v) or TFA/phenol/water/triisopropylsilane (88/5/5/2 v/v/v/v) and were purified to >95% purity by gradient HPLC (0.1% TFA/water with an acetonitrile gradient of 1%/min on a 1 × 25 cm Vydac C18 column). Masses were confirmed with a PE Sciex electrospray mass spectrometer or a MALDI-TOF mass spectrometer. Correct lactam formation was confirmed by amino acid sequencing. Cys residues were coupled by a modified procedure to avoid racemization. *N*-α-Fmoc-(*S*)-*p*-methoxytrityl-l-cysteine [Fmoc-Cys (Mmt)] was coupled with TBTU/HOBt (0.52 M) and 2.46 M collidine in DMF/DCM (1:1), as described by Han et al. (*22*). Disulfides were formed by iodine oxidation (*23*). The purified reduced peptide in 0.5 mL of HOAc/water (4:1) was treated with I_2 (10 equiv) for 15 h at room temperature. No Met or Trp oxidation was observed under these experimental conditions.

Bioassays. AC-stimulating activities of rat osteosarcoma (ROS 17/2) cells were determined as described previously (*24*). AC activities were expressed as percent of the maximum stimulation by hPTH(1−34)-NH_2 or [Leu^{27}]c-(Glu^{22}−Lys^{26})hPTH(1−31)NH_2 observed in a concurrent experiment. Data were averaged from a minimum of three independent experiments, and the data were fitted with a three-constant sigmoidal function (SigmaPlot, SPSS software). The ED_{50} value, the concentration of analogue that corresponds to the point of half-maximal stimulation, was then evaluated and the error was estimated from the corresponding fit to the error extremities for each data point.

Circular Dichroism Spectroscopy. Spectra were obtained on a Jasco J-600 spectropolarimeter at 20−22 °C. At least four spectra were averaged, and the data were smoothed by the Jasco software. The instrument was calibrated with ammonium (+)-10-camphorsulfonate. Peptides were dissolved in water, and sodium phosphate buffer, pH 7.2, was added to a final concentration of 25 mM. Peptide concentrations were calculated from the absorption at 280 nm, using an extinction coefficient of 5700 M^{-1}. Concentrations of hPTHrP analogues were determined from areas under the HPLC peak, with hPTH(1−31)NH_2 as reference standard. Data are expressed per peptide bond. Residues as α-helix were calculated from the value of θ_{222}, using a value of −28 000 deg·cm^2·$dmol^{-1}$ as the ellipticity per bond (*13*, *25*).

RESULTS

Lactams of [Leu^{27}]hPTH(1−31)NH_2. We have described previously the bioactivities of a cyclic analogue of hPTH-(1−31), [Leu^{27}]c(Glu^{22}−Lys^{26})hPTH(1−31)NH_2. This peptide has dramatically improved properties in both AC signaling and increasing of trabecular thickness in an ovariectomized rat model for osteoporosis (*17*, *19*, *26*). Recently, we reported that [Leu^{27}]c(Glu^{22}−Lys^{26})hPTH(1−

Table 1: Mass and AC-Stimulating Activities of Cyclic Analogues of hPTH

analogue	mass (observed)	mass (expected)	activity $ED_{50\%}$ (nM)
$[L^{27}]hPTH(1-31)NH_2$	3702.34[b]	3704.3	11.5 (±5.2)[a]
$[L^{27}]c(E^{22}-K^{26})hPTH(1-31)NH_2$	3685.46 (±0.46)	3685.1	7.5 (±0.6)
$[K^{22},E^{26},L^{27}]hPTH(1-31)NH_2$	3704.19[b]	3703.1	15.8 (±2.9)
$[K^{22},E^{26},L^{27}]c(K^{22}-E^{26})$ $hPTH(1-31)NH_2$	3684.84 (±0.47)	3685.1	6.5 (±0.3)
$[L^{27}]hPTH(1-29)NH_2$	3487.85 (±1.08)	3489.2	13.0 (±0.7)
$[L^{27}]c(E^{22}-K^{26})hPTH(1-29)NH_2$	3470.59 (±0.80)	3471.2	6.8 (±1.4)
$[L^{27}]hPTH(1-28)NH_2$	3360.75 (±0.51)	3361.1	19.1 (±3.1)
$[L^{27}]c(E^{22}-K^{26})hPTH(1-28)NH_2$	3342.63 (±0.50)	3341.8	8.3 (±1.0)
$[C^{22},C^{26},L^{27}]hPTH(1-31)NH_2$	3652.45 (±0.42)	3652.1	26.7 (±5.3)
$[C^{22},C^{26},L^{27}]c(C^{22}-C^{26})$ $hPTH(1-31)NH_2$	3649.71 (±0.61)	3650.1	15.9 (±0.7)
$[L^{27},E^{29}]hPTH(1-31)NH_2$	3704.19[b]	3704.1	21.5 (±1.1)
$[L^{27},K^{25},E^{29}]hPTH(1-31)NH_2$	3675.53[b]	3675.1	29.0 (±3.6)
$[L^{27},K^{25},E^{29}]c(K^{25}-E^{29})$ $hPTH(1-31)NH_2$	3659.3[b]	3658.1	35.8 (±9.0)
$[E^{17},L^{27}]hPTH(1-31)NH_2$	3745.0 (±0.52)	3745.2	13.9 (±2.8)
$[E^{17},L^{27}]c(K^{13}-E^{17})$ $hPTH(1-31)NH_2$	3727.30 (±0.30)	3727.2	12.3 (±2.5)
$[D^{17},L^{27}]c(K^{13}-D^{17},E^{22}-K^{26})$ $hPTH(1-31)NH_2$	3693.09 (±1.98)	3694.1	24.2 (±3.1)
$[E^{17},L^{27}]c(K^{13}-E^{17},E^{22}-K^{26})$ $hPTH(1-31)NH_2$	3709.60 (±0.46)	3710.4	8.0 (±0.7)

[a] Reference *17*. [b] Data from MALDI-TOF mass spectrum.

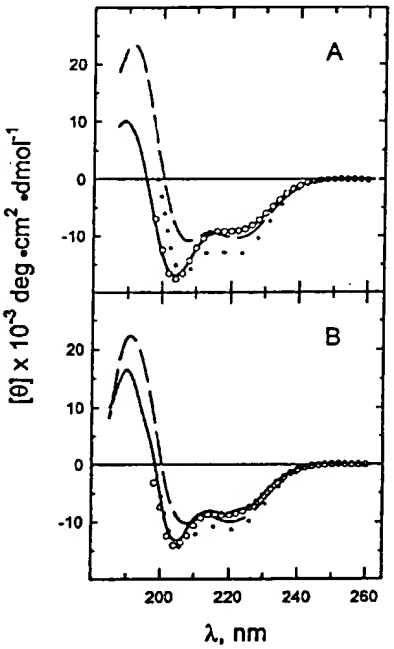

FIGURE 2: CD spectra of C-terminal deletion analogues of $[Leu^{27}]c(Glu^{22}-Lys^{26})hPTH(1-31)NH_2$. (A) Spectra of $hPTH(1-31)NH_2$, 119 μM (—) and 13 μM (O), and of [Leu27]c(Glu22–Lys26)hPTH(1–31)NH2, 123 μM (– –) and 12 μM (●). (B) Spectra of $[Leu^{27}]hPTH(1-28)NH_2$, 81 μM (—), of $[Leu^{27}]hPTH(1-28)NH_2$, 17 μM (O), and of $[Leu^{27}]c(Glu^{22}-Lys^{26})hPTH(1-28)NH_2$, 104 μM (– – –) and 16 μM (●).

$28)NH_2$ has AC-stimulating activity and osteogenic activity in the rat OVX model increased to levels comparable to $hPTH(1-31)NH_2$ or hPTH(1–34) (*20*). The AC-stimulating activities of $[Leu^{27}]c(Glu^{22}-Lys^{26})hPTH(1-29)NH_2$ and $[Leu^{27}]c(Glu^{22}-Lys^{26})hPTH(1-28)NH_2$ are shown in Table 1, and the CD spectrum of $[Leu^{27}]c(Glu^{22}-Lys^{26})hPTH(1-28)NH_2$ is shown in Figure 2. The effect of the cyclization and substitution of Leu-27 is to increase the AC-stimulating activity of the linear 1–28 and 1–29 analogues (*4*) about 5-fold to levels approaching that of $[Leu^{27}]c(Glu^{22}-Lys^{26})hPTH(1-31)NH_2$ (Table 1). It also dramatically increases the binding affinity of the 1–28 analogue for the human receptors expressed in porcine kidney cells (*20*). The corresponding CD spectra (Figure 2) demonstrate a substantial increase in α-helix, similar to that observed with $[Leu^{27}]c(Glu^{22}-Lys^{26})hPTH(1-31)NH_2$ compared to $hPTH(1-31)NH_2$ (*17*). The CD spectra of the cyclic analogues of these 28- and 29-residue analogues and of $[Leu^{27}]c(Glu^{22}-Lys^{26})hPTH(1-31)NH_2$ also show a pronounced concentration dependence, in contrast to the linear ones having a Leu-27 substitution (Figure 2). Thus, the concentration dependency must result from stabilization of the α-helix by the 22–26 lactam. The apparent amount of α-helix of the cyclized form at high concentration (104 μM), 10 residues, is actually less than observed at a lower concentration (16 μM), 11 residues, but the spectrum is much more like that of an ideal α-helix (*25*), as implied by the $\theta_{222}/\theta_{209}$ ratio being closer to 1. These data are consistent with a relatively restricted region of the sequence having a conformation closer to the idealized α-helix. A theoretical study has demonstrated that the CD spectrum is highly sensitive to the φ, ψ angles of the peptide and that a minimum of 7 residues in an α-helical configuration is necessary to give its idealized spectrum (*27*). These considerations suggest that residues 17–28 are stabilized as α-helix by the presence of the lactam. This analysis ignores the weak contribution of the rest of the molecule to $[\theta]_{222}$. Although NMR evidence indicates a short α-helix between residues 3 and 9 in hPTH(1–37) or hPTH(1–34) (*28*), no evidence was found for this structure in the CD spectra of hPTH fragments, particularly hPTH(1–19) (*13*). The lack of CD evidence for this short helix is consistent with the known dependency of helical signal per residue on the number of helical residues (*25*). Helices shorter than about nine residues are not expected to have any characteristic helical spectrum (*27*). The dimerization likely has no importance in terms of PTH function because the concentration at which it is observed is at least 1000-fold higher than biological concentrations. However, it can lead to misinterpreting spectral results in terms of biologically important conformations. Two further possible complications exist in interpreting the CD spectra. These are possible contributions of the single Trp near 225 nm and a contribution from the lactam. In earlier work, we found a strong CD in the 230–300 nm spectral range in the lactam analogue $c(Lys^{26}-Asp^{30})$-

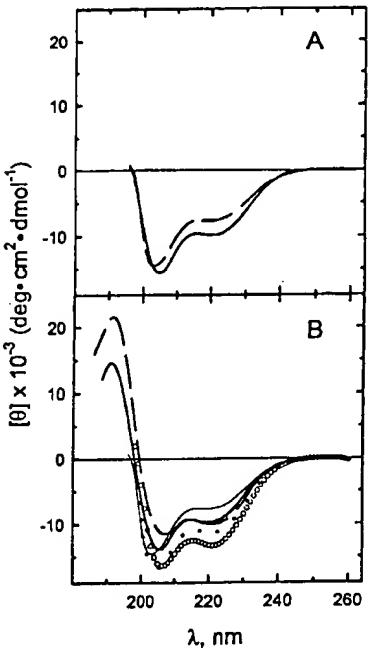

FIGURE 3: (A) CD spectrum of [Lys^{22},Glu^{26},Leu^{27}]hPTH(1−31)-NH_2 at 12 μM (− − −) compared with that of [Leu^{27}]hPTH-(1−31)NH_2 at 13 μM (—). (B) CD spectra of [Lys^{22},Glu^{26},Leu^{27}]c-(Lys^{22}−Glu^{26})hPTH(1−31)NH_2 at 84 μM (− − −) and 12 μM (●) and of [Lys^{22},Glu^{26},Leu^{27}]hPTH(1−31)NH_2 at 82 μM (thick solid line) and 15 μM (thin solid line). The spectrum of [L^{27}]c-(E^{22}−K^{26})hPTH(1−31)NH_2 at 12 μM has also been included for comparison (○).

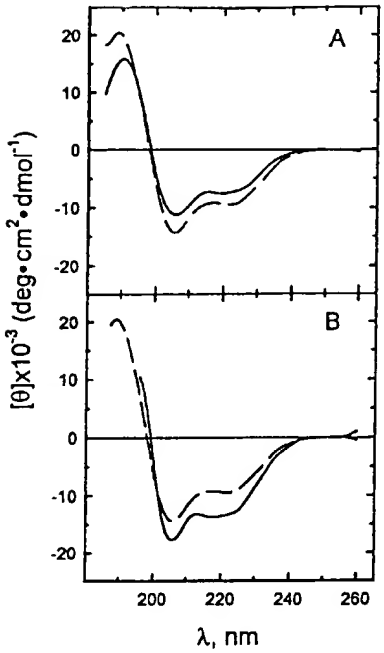

FIGURE 4: (A) CD spectra of [Leu^{27}]hPTH(1−31)NH_2, 95 μM (—), and of [Lys^{25},Leu^{27},Glu^{29}]hPTH(1−31)NH_2, 60 μM (− − −). (B) CD spectra of [Lys^{25},Leu^{27},Glu^{29}]hPTH(1−31)NH_2, 60 μM (− − −), and of [Lys^{25},Leu^{27},Glu^{29}]c(Lys^{25}−Glu^{29})hPTH(1−31)-NH_2 at 47 μM (—).

hPTH(20−34)NH_2 (*18*). However, we did not find a significant spectrum when we later examined [Leu^{27}]c(Glu^{22}−Lys^{26})hPTH(1−31)NH_2. One model for the single lactam contribution is the CD of alkyl β-lactams (*29*). The possible contribution, using this model, is less than 200 deg cm^2/dmol at 220 nm. We have ignored both of these contributions as minor ones that do not affect the conclusions derived from the spectra.

In an earlier study with a multicyclic polypeptide model compound, Ösapay and Taylor (*30*) reported that Lys^i,Glu^{i+4} lactams were only weakly helix-stabilizing, in contrast to Glu^i,Lys^{i+4} ones. The analogue [Lys^{22},Glu^{26},Leu^{27}]c(Lys^{22}−Glu^{26})hPTH(1−31)NH_2 is the same as [Leu^{27}]c(Glu^{22}−Lys^{26})hPTH(1−31)NH_2 but with residues 22 and 26 reversed (Figure 1). This analogue had the same AC-stimulating activity as [Leu^{27}]c(Glu^{22}−Lys^{26})hPTH(1−31)NH_2 (Table 1). When both were measured at similar low concentrations, the CD spectra showed that the linear analogue is less helical, as judged by its θ_{222} value (θ_{222} = −7500) and a blue shift from 205 to 203 nm of the lower wavelength minimum, compared to [Leu^{27}]hPTH(1−31)NH_2 (θ_{222} = −9800) (Figure 3A). In either analogue, ionic interactions between the Glu-22 and Lys-26 side chains are expected to stabilize the α-helix by about 0.5 kcal/mol (*31*). However, the effect of interchanging the Glu-22 and Lys-26 residues is to lose the stabilization of the Ser-17 to Gln-29 α-helix (*12*) resulting from the side-chain interactions of Glu-22 and Lys-26 with the helix macrodipole (*32, 33*). The CD spectra of both the linear and cyclic analogues of [Lys^{22},Glu^{26},Leu^{27}]hPTH(1−31)NH_2 at low and high concentrations indicated a change in conformation to a more helical form at higher concentrations, presumably as a result of dimerization. Comparison of the two 22−26 lactams at the 12 μM concentration showed that the Lys-22 to Glu-26 cyclized analogue had less α-helix (about 12 residues) than the corresponding analogue with the natural sequence (about 14 residues), similar to earlier observations with model peptides (*30*).

Two lactams of i, i + 4 spaced residues can be formed from the native sequence of PTH, between residues 22 and 26 or residues 26 and 30. Only the analogue with a lactam between residues 22 and 26 had an enhanced AC-stimulating activity (*17*), presumably because it stabilizes a conformation closer to that of the receptor-bound one. If one assumes that residues 21−29 bind with the hydrophobic face of the amphiphilic α-helix interacting with the receptor, then an analogue that has a lactam formed between appropriately substituted residues 25 and 29 of the hydrophilic face should have at least comparable activity to the native sequence. The linear analogue [Lys^{25},Leu^{27},Glu^{29}]hPTH(1−31)NH_2, with an $ED_{50\%}$ of 29 nM, was much less active than [Leu^{27}]hPTH-(1−31)NH_2 ($ED_{50\%}$ 11.5 nM) (Table 1). The lactam analogue [Leu^{27},Lys^{25},Glu^{29}]c(Lys^{25}−Glu^{29})hPTH(1−31)NH_2 had slightly less activity ($ED_{50\%}$ 36 nM) than the linear analogue, similar to the effect of cyclization between residues 26 and 30 (*17*). CD spectra comparing [Leu^{27}]hPTH(1−31)NH_2 and [Lys^{25},Leu^{27},Glu^{29}]hPTH(1−31)NH_2 indicated the latter had more α-helix than the former (Figure 4A), as expected. The mutations Arg25Lys and Gln29Glu are neutral in terms of their single amino acid α-helix stabilizing effects (*34*). However, there are two other competing effects on helical stability resulting from the substitution of Glu for Gln at position 29. The substitution has a negative effect on the stability of the helix resulting from an unfavorable interaction with the helix macrodipole and a positive effect resulting

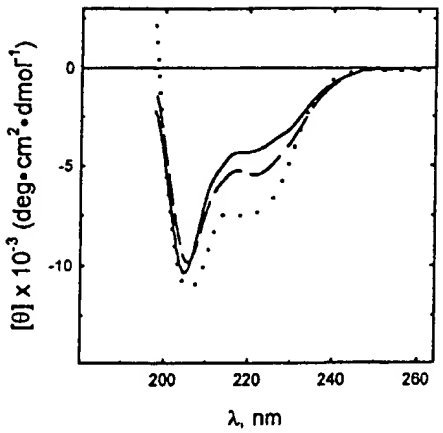

FIGURE 5: CD spectra of [Cys[22],Cys[26],Leu[27]]hPTH(1−31)NH_2, 22 μM (− − −), and of [Cys[22],Cys[26],Leu[27]]c(Cys[22]−Cys[26])hPTH-(1−31)NH_2, 20 μM (—). The spectrum of [Leu[27]]hPTH(1−31)-NH_2 (●) is shown for comparison.

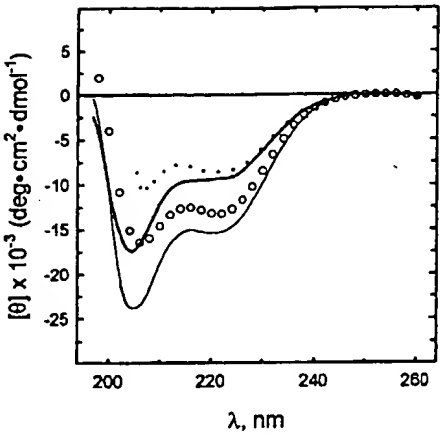

FIGURE 6: CD spectra of [Glu[17],Leu[27]]hPTH(1−31)NH_2, 12 μM (thin solid line), of [Glu[17],Leu[27]]c(Lys[13]−Glu[17])hPTH(1−31)NH_2, 12 μM (thick solid line), of [Glu[17],Leu[27]]c(Lys[13]···Glu[17],Glu[22]−Lys[26])hPTH(1−31)NH_2, 2.6 μM (●), and of [Leu[27]]c(Glu[22]−Lys[26])-hPTH(1−31)NH_2, 12 μM (●).

from a favorable ion-pair stabilization between Lys-25 and Glu-29. Ion pairs between i, $i + 4$ spaced residues have been reported to stabilize α-helices (*16*) by about −0.5 kcal/mol (*31*, *35*). This latter effect is the most important (*32*), resulting in a net stabilization of the α-helix (Figure 4A). Lactam formation resulted in increased α-helix, with 14 residues estimated as α-helix in the cyclic form and 10 in the linear (Figure 4B). The loss of activity seen in the linear analogue suggests that one or both of residues 25 and 29 have at least some interaction with the receptor, and the similar AC stimulation by the cyclic analogue suggests that the conformational constraint afforded by this cyclization is not specifically favorable to receptor binding. Solution structures from NMR data show that the side chains of Arg-25 and Gln-29 are spaced at least 10 Å apart (*28*). If these conformations reflect the receptor-bound one, then lactam constraint would not be expected to have a positive effect on receptor activation, as was observed (Table 1).

Cystine Analogues of hPTH(1−31)NH_2. The lactam analogue [Leu[27]]c(Glu[22]−Lys[26])hPTH(1−31)NH_2 has 21 atoms forming its ring, which, although stabilizing an α-helix in the region of the cyclization, still permits considerable conformational freedom. The corresponding cyclic analogue formed when residues 22 and 26 are mutated to Cys and then cyclized contains only 17 atoms in the ring, thus permitting fewer degrees of freedom. The linear analogue, [Cys[22],Cys[26],Leu[27]]hPTH(1−31)NH_2, has less activity than [Leu[27]]hPTH(1−31)NH_2. Cyclization of the molecule by oxidation to give [Cys[22],Cys[26],Leu[27]]c(Cys[22]−Cys[26])hPTH-(1−31)NH_2 significantly increased its activity, from an $ED_{50\%}$ of about 27 nM to 16 nM (Table 1). Replacement of the Glu-22 and Lys-26 residues with Cys is expected to substantially reduce the α-helix stability, according to a structure-based scale of α-helix propensities of amino acids (*36*). This is in agreement with the relative CD spectra of [Leu[27]]hPTH(1−31)NH_2 and [Cys[22],Cys[26],Leu[27]]hPTH(1−31)NH_2, the former having eight residues in α-helix compared to about six residues in the latter. Surprisingly, comparison of the CD spectra of the linear and cyclic Cys-22, Cys-26 analogues indicated little difference in their conformations, the linear form having a slightly greater helical content than the cyclic (Figure 5).

Double Cyclic Analogue of [Leu[27]]hPTH(1−31)NH_2. The monocyclic analogue [Glu[17],Leu[27]]c(Lys[13]−Glu[17])hPTH(1−31)NH_2 had about the same activity compared to the linear analogue, in contrast to the increased activity observed in the monocyclic Glu-22 to Lys-26 analogue (Table 1). The double cyclic analogue [Glu[17],Leu[27]]c(Lys[13]−Glu[17],Glu[22]−Lys[26])hPTH(1−31)NH_2 had an activity similar to that of [Leu[27]]c(Glu[22]−Lys[26])hPTH(1−31)NH_2. The CD spectra of [Glu[17],Leu[27]]hPTH(1−31)NH_2, [Glu[17],Leu[27]]c(Lys[13]−Glu[17])-hPTH(1−31)NH_2, [Glu[17],Leu[27]]c(Glu[22]−Lys[26])hPTH(1−31)-NH_2, and [Glu[17],Leu[27]]c(Lys[13]−Glu[17],Glu[22]−Lys[26])hPTH-(1−31)NH_2 are shown in Figure 6. [Glu[17],Leu[27]]hPTH-(1−31)NH_2 is substantially more α-helical than [Leu[27]]-hPTH(1−31)NH_2, having an estimated 16 α-helical residues as opposed to 11. Since the Ser17Glu substitution is expected to be neutral in terms of helix stability (*34*, *36*), we surmise that the source of stability for the additional α-helix may be the ionic interaction from the side chains of Lys-13−Glu-17, which is absent in the natural sequence. The spectrum of [Glu[17],Leu[27]]c(Glu[22]−Lys[26])hPTH(1−31)NH_2 was very similar to that of [Leu[27]]c(Glu[22]−Lys[26])hPTH(1−31)NH_2 (data not shown). The spectrum of [Glu[17],Leu[27]]c(Lys[13]−Glu[17])hPTH(1−31)NH_2 is similar in shape to but less intense than the spectrum of its linear form and is clearly less helical, as indicated by its $[\theta]_{222}$ value and $[\theta]_{222}/[\theta]_{209}$, than the corresponding analogue where cyclization is between residues 22 and 26. All spectra are at concentrations from 7 to 12 μM, where there is negligible aggregation. The spectrum of the double cyclic is not the sum of the two monocyclics, suggesting an interaction between the two cyclic regions. Its apparent α-helix content, from the $[\theta]_{222}$ value, is about the same as that of the 13−17 lactam analogue but significantly less than that of the 22−26 lactam analogue. The shape of its spectrum is, however, much more α-helical than that of either analogue with the single lactam. NMR data have indicated that PTH has a bend in the region of Lys-13 to Ser-17 (*37*), and this makes the interpretation of the CD results somewhat complicated. Turn structures can have CD spectra somewhat similar to that observed with α-helices, with a weak negative band at 225 nm but with a positive ellipticity near 209 nm (*38*).

Table 2: Mass and AC-Stimulating Activities of Cyclic Analogues of hPTHrP

analogue	mass (observed)	mass (expected)	activity $ED_{50\%}$ (nM)
$hPTHrP(1-31)NH_2$	3707.26 (±0.27)	3707.3	21.4 (±1.3)
$[E^{22},K^{26}]hPTHrP(1-31)NH_2$	3680.38 (±0.31)	3679.1	8.2 (±0.9)
$[E^{22},K^{26}]c(E^{22}-K^{26})$ $hPTHrP(1-31)NH_2$	3661.31 (±0.41)	3662.3	10.2 (±2.5)
$[K^{26}]hPTHrP(1-31)NH_2$	3698.14 (±0.47)	3698.1	7.7 (±2.1)
$[K^{26}]c(K^{26}-E^{30})$ $hPTHrP(1-31)NH_2$	3679.93 (±0.78)	3680.1	14.6 (±2.0)

Cyclic Analogues of PTHrP. PTHrP(1−31) also has an amphiphilic helical sequence between residues 21 and 31, which we have postulated binds to the receptor in a manner similar to the binding of the PTH amphiphilic helix (*4*). If so, cyclizations on the polar face could have similar effects on α-helix stabilization and AC stimulation to those observed with PTH. To test this possibility, we synthesized $[Glu^{22},Lys^{26}]hPTHrP(1-31)NH_2$ and $[Lys^{26}]hPTHrP(1-31)NH_2$ and their cyclic analogues, $[Glu^{22},Lys^{26}]c(Glu^{22}-Lys^{26})hPTHrP(1-31)NH_2$ and $[Lys^{26}]c(Lys^{26}-Glu^{30})hPTHrP(1-31)NH_2$ (Figure 1B). The AC-stimulating activities of these analogues as compared to the native hPTHrP are shown in Table 2. Both of the linear analogues, $[Glu^{22},Lys^{26}]hPTHrP(1-31)NH_2$ and $[Lys^{26}]hPTHrP(1-31)NH_2$, are more active than the natural sequence $hPTHrP(1-31)NH_2$.Lactam formation diminished the AC-stimulating activity of each of these linear analogues, with $[Glu^{22},Lys^{26}]hPTHrP(1-31)NH_2$ having about 80% of the activity of the linear form and $[Lys^{26}]hPTHrP(1-31)NH_2$ having about 50% of the activity of the linear one. Thus, relative activities of the two cyclic analogues were similar to those observed with hPTH, but neither improved the activity of the corresponding linear one.

The CD spectra of both of the cyclic analogues, $[Glu^{22},Lys^{26}]c(Glu^{22}-Lys^{26})hPTHrP(1-31)NH_2$ and $[Lys^{26}]c(Lys^{26}-Glu^{30})hPTHrP(1-31)NH_2$, are clearly more α-helix-like, in terms of the ratios of ellipticities at 222 and 209 nm, than the linear forms (Figure 7). Despite this, the $[\theta]_{222}$ values for the linear and cyclized Glu-22−Lys-26 analogues are very similar. There is no evidence for concentration-dependent dimerization of this $Glu^{22}-Lys^{26}$ cyclic analogue (Figure 7A), but there is evidence for dimerization of $[Lys^{26}]c(Lys^{26}-Glu^{30})hPTHrP(1-31)NH_2$ (Figure 7B). In this case, the spectrum shows a characteristic increase in the $[\theta]_{222}$ value and approach of the $[\theta]_{209}/[\theta]_{222}$ ratio toward 1, typical of formation of α-helix, as the concentration increases. The linear analogue $[K^{26}]hPTHrP\text{-}NH_2$ has less α-helix than $[Glu^{22},Lys^{26}]hPTHrP(1-31)NH_2$ but more than its cyclized analogue, $[Lys^{26}]c(Lys^{26}-Glu^{30})hPTHrP\text{-}NH_2$. The spectra suggest cyclization results in a localized α-helix in the region of the lactam but an overall diminishing of helix in the molecule. The data further imply the receptor-binding structure of hPTHrP(1−31) is not α-helical near its C-terminus, similar to hPTH(1−31), but is helical, but perhaps not perfectly α-helical, in the region defined by the 22−26 lactam.

It is noteworthy that whereas hPTH has natural salt bridges that occur between residues 22 and 26 or residues 26 and 30 when this region of PTH is in an α-helical conformation, no such bridges are present in hPTHrP. In fact, $hPTHrP(21-31)NH_2$, unlike $[Leu^{27}]hPTHrP(21-31)NH_2$ or even the wild-type sequence $hPTH(21-31)NH_2$, is not amphiphilic and α-helical simultaneously. This is shown in Figure 8,

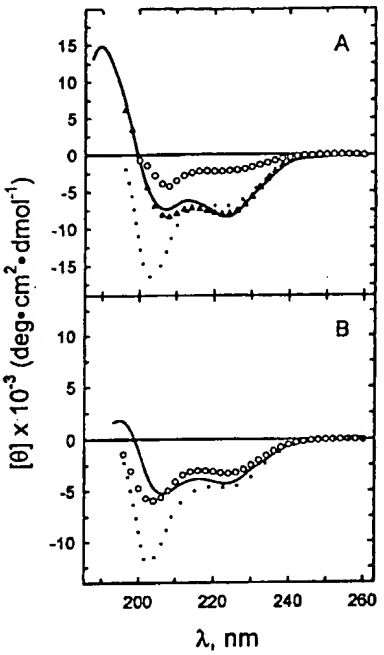

FIGURE 7: CD spectra of cyclic analogues of $hPTHrP(1-31)NH_2$. (A) Spectra of $[Glu^{22},Lys^{26}]hPTHrP(1-31)NH_2$, 14 μM (●), of $[Glu^{22},Lys^{26}]c(Glu^{22}-Lys^{26})hPTHrP(1-31)NH_2$, 68 μM (—) and 14 μM (▲), and of $hPTHrP(1-31)NH_2$, 14 μM (O). (B) Spectra of [Lys26]hPTHrP(1−31)NH2, 14 μM (●), and of $[Lys^{26}]c(Lys^{26}-Glu^{30})hPTHrP(1-31)NH_2$, 68 μM (—) and 14 μM (O).

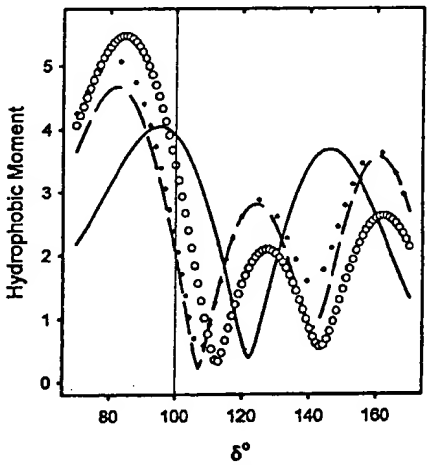

FIGURE 8: Hydrophobic moments (*39*) for C-terminal helical region of hPTH and hPTHrP. For an ideal α-helix, δ is 100°. Calculated moments are shown for the following peptides, with the value of δ for the maximum nearest 100° in parentheses: hPTH(21−31) (95°), (—); hPTHrP(21−31) (82°), (− − −); $[Glu^{22},Lys^{26}]hPTHrP(21-31)$ (84°), (O); and $[Lys^{26}]hPTHrP(21-31)$ (81°), (●)

where the hydrophobic moment is calculated as a function of helical angle (*39*). For an ideal amphiphilic α-helix, this function has a maximum at 100°. The native sequence of $hPTHrP(21-31)NH_2$ has a maximum moment at 82°, well displaced from that of 97° for $[Leu^{27}]hPTH(21-31)NH_2$ or 96° for $hPTH(21-31)NH_2$.

DISCUSSION

When a peptide, such as PTH, binds to its receptor, there is a large entropic penalty due to loss of translational and

rotational degrees of freedom of the peptide (*40*). The overall loss of entropy is partly diminished by the presence of internal vibrational modes in the complex not present in the unbound peptide (*41, 42*). The remaining contributions to a favorable free energy of binding are assumed to result from a favorable enthalpy of binding and entropic contributions from the hydrophobic effect, including a favorable entropic effect from the release of bound water from the nonpolar side chains that become buried on complex formation. Entropy-driven binding has been observed, for example, in ligand binding to the δ-opoid receptor (*43*). Water release has been shown to result in both favorable enthalpic and entropic contributions, depending on the system (*44*). Detailed studies with human growth hormone and its receptor have shown that both enthalpic and entropic effects can determine favorable binding (*45*).

Regardless of the compensatory mechanisms to overcome the unfavorable entropy change on receptor binding, a suitable constraint of the peptide will increase receptor binding by limitation of the degrees of freedom of the free peptide. Such a cyclization must limit the conformations of the peptide to a subset that includes the productively bound conformations of the hormone. Early work indicated α-helices are stabilized by Glu···Lys$^+$ *i*, *i* + 4 spaced salt bridges, although not *i*, *i* + 3 spaced ones (*16*). Later work with amphiphilic model peptides showed that lactams between residues spaced *i*, *i* + 4 indeed stabilized the helices, but this depended on the location and orientation of the residues. Thus, Glu−Lys lactams were helix-stabilizing but Lys−Glu ones destabilized the α-helical conformation (*46*). In pioneering work, Felix et al. (*47*) applied lactam stabilization to growth hormone-releasing factor (GRF), where they reported that an analogue containing a lactam between residues 8 and 12 had a long α-helical segment and improved bioactivity. These workers reported the structure of cyclic analogues between residues Asp-8 and Lys-12 and residues Lys-21 and Asp-25. In both instances α-helices near the N-terminus and C-terminus were stabilized by the lactams (*48*). Although GRF and PTH share certain structural features, including size, the location of their helices, and an amphiphilic helical sequence near their C-termini, the two hormones share no sequence similarity. The reason for their apparent structural similarities became clear after their respective receptors had been isolated and shown to belong to a common family (*1*).

Initially, we focused on lactam formation between natural possible ion pairs: residues 22 and 26, 26 and 30, and 27 and 30. Our work on these lactam-containing analogues situated in the osteogenically active fragment [Leu^{27}]hPTH-(1−31)NH_2 demonstrated that only the lactam between residues 22 and 26 led to both increased AC-stimulating and osteogenic activities (*17, 19*). As shown here, the residues can be reversed without significantly affecting AC-stimulating activity. Although it has been reported that Lys−Glu orientations did not induce α-helix in a model peptide (*46*), the effect observed depends on the context of the lactam. Kapurniotu and Taylor (*49*) observed that only a Lys−Asp lactam induced α-helix among the three lactams of calcitonin they examined, and Fry et al. (*48*) reported local helix stabilization in a GRF analogue having a lactam between Lys-21 and Asp-25. We did not observe any difference between the CD spectra of the lactams when the pairs were Glu-22−Lys-26 or Lys-22−Glu-26 at the highest concentrations (about 80 μM). However, spectra taken at a lower concentration (about 15 μM) did show a small difference (Figure 3). One could argue that the situation at the higher concentration, where there is likely dimerization, is perhaps closer to that expected for the receptor-bound hormone. Regardless, helix stabilization is associated with higher agonist activity.

The Cys-22−Cys-26 cyclic analogue was prepared to study the effect of reduction of ring size, in this case from 21 atoms for the Glu−Lys lactam to 17 for the Cys−Cys one. AC-stimulating activitiy was diminished by presence of the double Cys mutation but partially overcome by cyclization. The loss of helix in the linear analogue, observed in the CD spectrum, is expected from known amino acid helix propensities (*50*). There was no helical stabilization, in comparison with either the linear [Cys^{22},Cys^{26},Leu^{27}]hPTH(1−31)NH_2 or [Leu^{27}]hPTH(1−31)NH_2, as a result of ring formation (Figure 5). This interpretation assumes that there is no contribution of the cystine to the far-UV CD. A recent study of bovine pancreatic trypsin inhibitor indicated that no correction to the CD spectrum was necessary in this wavelength region for a disulfide contribution (*51*). However, it should be noted that there are uncertainties in the interpretation of the CD data of our Cys analogues. A theoretical study has demonstrated that the intensity of the CD is quite sensitive to the specific ϕ, ψ angles present (*27*), and the constraint of the smaller ring may yield a helix, but with a different geometry than with the lactam. Loss of activity, similar to that observed here, has been reported with human growth hormone releasing hormone, which activates a PTH-related receptor, on replacing an Asp-25−Orn-29 lactam with a Cys−Cys ring (*52*). Interpretation of these changes in ring size requires that the effect of the substitutions in the linear analogue also be considered, and this has not always been done in studies reported in the literature.

Cyclization with a lactam between residues 13 and 17 of hPTHrP(1−34) was observed to enhance AC stimulation of a human osteosarcoma cell line, SaOS-2/B-10, by a factor of about 3, and this activity enhancement was retained in a double cyclized 13−17/26−30 analogue even though the 26−30 analogue itself was much less active than the linear PTHrP (*53*). Double cyclic analogues of hPTH(1−31)NH_2, having 13−17 and 26−30, 13−17 and 18−22, or 18−22 and 26−30 lactams were described very recently (*54*). Their results suggested only a bicyclic analogue with 18−22 and 22−26 lactams had increased activity relative to the linear analogue. A double cyclic analogue of PTHrP(7−34)NH_2, with side-chain lactams between residues 13 and 17 and residues 26 and 30, has been reported to have increased antagonist activity compared to the linear parent (*53*). In our work, AC stimulation of ROS 17/2 cells by [Glu^{17},Leu^{27}]c(Lys^{13}−Glu^{17})hPTH(1−31)NH_2 was approximately the same as that of the linear analogue. However, enhancement was increased in [Glu^{17},Leu^{27}]c(Lys^{13}−Glu^{17},Glu^{22}−Lys^{26})hPTH-(1−31)NH_2. The Asp-17 analogue, [Asp^{17},Leu^{27}]c(Lys^{13}−Asp^{17},Glu^{22}−Lys^{26})hPTH(1−31)NH_2, had diminished activity, presumably due to the restriction of the smaller ring size of the first cyclization (Table 1). Our CD results of Figure 6 show that the structure of the double cyclic mutant [Glu^{17},-Leu^{27}]c(Lys^{13}−Glu^{17})hPTH(1−31)NH_2 is not a simple sum of the structures of the two single cyclic analogues. A similar

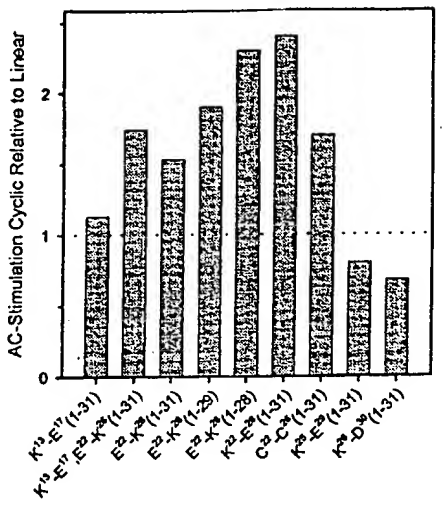

FIGURE 9: Ratios of AC-stimulating activities of cyclic to corresponding linear analogues of hPTH.

observation was reported in an earlier NMR and CD study of mono- and bicyclic analogues of GRF, a hormone that binds to a PTH-related receptor (*48*). Presumably, this is because the peptide regions bounded by the lactams interact with one another.

Although these data indicate that the region bounded by residues 21 and 27 binds to the receptor as an α-helix, the binding conformation of the C-terminal region from about residue 26 to 31 is most likely some type of distorted helix. Analogues that are cyclized in this region either have no increased activity as a result of cyclization, such as [Leu^{27}]c(Lys^{26}−Asp^{30})hPTH(1−31)NH$_2$ (*17*), or have lowered activity, as observed with the analogue [Lys^{25},Leu^{27},Glu^{29}]c(Lys^{25}−Glu^{29})hPTH(1−31)NH$_2$ reported here. From these data, PTH seems to bind to the receptor as an α-helix between about residues 21 and 27 and a more extended helix, or at least a distorted one, from about residue 27 to the C-terminus, residue 31. We observed no enhancement of activity on constraint of residues 13−17 alone. Since there is a bend in linear PTH in this region, interpretation of the CD data is difficult. Figure 9 summarizes the relative activities of constrained versus linear analogues. It shows clearly that only the region from about residues 21 to 27 likely is in a true α-helix conformation.

Our conclusions concerning the effect of cyclization on the AC agonist activity of PTH are largely compatible with the data recently reported by Condon et al. (*54*). They found a modest effect of cyclization between residues 13 and 17 on AC stimulation and a strong effect of a midregion cyclization, between residues 18 and 22, similar to the effect observed by us between residues 22 and 26. There was no additional enhancement of activity, relative to that of the 18−22 monocyclic analogue, with the 13−17/22−26 bicyclic analogue, but there appeared to be some additional activity when the 26−30 region was cyclized in addition to the 18−22 cyclization. However, their conclusions on the receptor-bound conformation of PTH are not quite consistent with our data. They concluded that hPTH(1−31) binds to the receptor as one continuous helix, rather than the helix−bend−helix inferred from numerous NMR studies on the solution structure of PTH. To circumvent the low solubility of the double lactam analogues, they performed their experiments at pH ~3.6 and in 20% acetonitrile. Under these conditions, they obtained a strong CD signal with the tricyclic analogue, which indicated this molecule was fully α-helical. In addition, their experiments were performed at a concentration of 40 μM, a level at which we observe dimerization leading to increased helix in some cyclic analogues. Solubility of our double cyclic PTH analogues was also a problem, necessitating the use of very dilute solutions. Acetonitrile has been reported to induce α-helix in both model and natural peptides (*55*, *56*), and we suggest this difference in solvent conditions and peptide concentrations likely explains the difference in our results. It should also be noted that their reported spectrum for hPTH(1−31)NH$_2$ is very much more intense, having a $[\theta]_{222}$ of −19 300 compared to our previously reported value of −7500 in neutral, aqueous buffer (17). We cannot absolutely rule out the possibility that PTH binds as a continuous helix, but we believe the preponderance of data at this time is more indicative of it binding with some bend near its midregion.

The activity and CD data reported here on similar analogues of hPTHrP(1−31)NH$_2$ are similar overall to the observations with hPTH. However, there is no clear enhancement of AC stimulation by lactam formation between residues 22 and 26 as is seen with PTH. A recent NMR study of hPTHrP(1−34) indicated that this molecule has two helices, a short one between His-5 and Asp-10 and a longer C-terminal one between residues Ser-14 and Ala-29, connected by a flexible segment (*37*). As shown by their CD spectra, cyclized [Glu^{22},Lys^{26}]hPTHrP(1−31)NH$_2$ had greater α-helix than the linear sequence and cyclized [Lys^{26}]hPTHrP(1−31)NH$_2$ had less helical content than the linear one (Figure 7). In either case, lactam formation constrained a portion of the molecule to α-helix, as evidenced by the θ_{222} values and particularly by the ratios $\theta_{209}/\theta_{222}$. There is evidence from receptor interaction studies of PTH/PTHrP hybrids that the residue 21−34 region of the two species can be substituted independently and activate the receptor and also that their 15−34 domains have similar receptor affinities (*57*). This, along with knowledge that certain residues on the hydrophobic face of the C-terminal α-helix of hPTH are critical for receptor binding and activation, implies that the PTHrP must adopt a somewhat similar configuration to activate the receptor. The AC activation and CD data presented here suggest that the conformation of PTHrP bound to the receptor is likely a somewhat distorted helix that would permit optimal interaction of its C-terminal hydrophobic residues with the receptor and not the perfect one that seems to characterize bound PTH in the 21−27 residue region.

ACKNOWLEDGMENT

We thank D. Krajcarski for mass spectra.

REFERENCES

1. Jüppner, H., Abou Samra, A. B., Freeman, M., Kong, X. F., Schipani, E., Richards, J., Kolakowski, L. F., Jr, Hock, J., Potts, J. T., Jr., Kronenberg, H. M., and Segre, G. V.(1991) *Science 254*, 1024−1026.
2. Rixon, R. H., Whitfield, J. F., Gagnon, L., Isaacs, R. J., Maclean, S., Chakravarthy, B., Durkin, J. P., Neugebauer, W.,

Ross, V., Sung, W., and Willick, G. E. (1994) *J. Bone Miner. Res. 9*, 1179−1189.
3. Tregear, G. T., Van Rietschoten, J., Greene, E., Keutmann, H. T., Niall, H. D., Reit, B., Parsons, J. A., and Potts, J. T., Jr. (1973) *Endocrinology 93*, 1349−1353.
4. Neugebauer, W., Barbier, J. R., Sung, W. L., Whitfield, J. F., and Willick, G. E. (1995) *Biochemistry 34*, 8835−8842.
5. Whitfield, J. F., Morley, P., Willick, G. E., MacLean, S., Ross, V., Barbier, J., and Isaacs, R. J. (1999) *Calcif. Tissue Int. 65*, 143−147.
6. Stewart, A. F. (1996) *Bone 19*, 303−306.
7. Whitfield, J. F., Morley, P., Willick, G. E., Ross, V., Langille, R., MacLean, S., Barbier, J., Isaacs, R. J., and Ohannessian Barry, L. (1997) *Calcif. Tissue Int. 61*, 322−326.
8. Pausova, Z., Bourdon, J., Clayton, D., Mattei, M. G., Seldin, M. F., Janicic, N., Riviere, M., Szpirer, J., Levan, G., Szpirer, C., Goltzman, D., and Hendy, G. N. (1994) *Genomics 20*, 20−26.
9. Caulfield, M. P., McKee, R. L., Goldman, M. E., Duong, L. T., Fisher, J. E., Gay, C. T., DeHaven, P. A., Levy, J. J., Roubini, E., Nutt, R. F., Chorev, M., and Rosenblatt, M. (1990) *Endocrinology 127*, 83−87.
10. Klaus, W., Dieckmann, T., Wray, V., Schomburg, D., Wingender, E., and Mayer, H. (1991) *Biochemistry 30*, 6936−6942.
11. Barden, J. A., and Kemp, B. E. (1993) *Biochemistry 32*, 7126−7132.
12. Marx, U. C., Austermann, S., Bayer, P., Adermann, K., Ejchart, A., Sticht, H., Walter, S., Schmid, F. X., Jaenicke, R., Forssmann, W.-G., and Rösch, P. (1995) *J. Biol. Chem. 270*, 15194−15202.
13. Neugebauer, W., Surewicz, W. K., Gordon, H. L., Somorjai, R. L., Sung, W., and Willick, G. E. (1992) *Biochemistry 31*, 2056−2063.
14. Gardella, T. J., Wilson, A. K., Keutmann, H. T., Oberstein, R., Potts, J. T., Kronenberg, H. M., and Nussbaum, S. R. (1993) *Endocrinology 132*, 2024−2030.
15. Surewicz, W. K., Neugebauer, W., Gagnon, L., MacLean, S., Whitfield, J. F., and Willick, G. E. (1993) in *Peptides: Chemistry, Structure, and Biology* (Hodges, R., and Smith, J., Eds.) pp 556−558, Proceedings of 13th American Peptide Symposium, ESCOM, Leiden, The Netherlands.
16. Marqusee, S., and Baldwin, R. L. (1987) *Proc. Natl. Acad. Sci. U.S.A. 84*, 8898−8902.
17. Barbier, J. R., Neugebauer, W., Morley, P., Ross, V., Soska, M., Whitfield, J. F., and Willick, G. (1997) *J. Med. Chem. 40*, 1373−1380.
18. Neugebauer, W., Gagnon, L., Whitfield, J., and Willick, G. E. (1994) *Int. J. Pept. Protein Res. 43*, 555−562.
19. Whitfield, J. F., Morley, P., Willick, G., Langille, R., Ross, V., Maclean, S., and Barbier, J. R. (1997) *J. Bone Miner. Res. 12*, 1246−1252.
20. Whitfield, J. F., Morley, P., Willick, G. E., Isaacs, R. J., MacLean, S., Ross, V., Barbier, J. R., Divieti, P., and Bringhurst, F. R. (2000) *J. Bone Miner. Res 15*, 964−970.
21. Fields, G. B., and Noble, R. L. (1990) *Int. J. Pept. Protein Res. 35*, 161−214.
22. Han, Y., Albericio, F., and Barany, G. (1997) *J. Org. Chem. 62*, 4307−4312.
23. Annis, I., Hargittai, B., and Barany, G. (1997) *Methods Enzymol. 289*, 198−221.
24. Jouishomme, H., Whitfield, J. F., Gagnon, L., Maclean, S., Isaacs, R., Chakravarthy, B., Durkin, J., Neugebauer, W., Willick, G., and Rixon, R. H. (1994) *J. Bone Miner. Res. 9*, 943−949.
25. Yang, J. T., Wu, C. S., and Martinez, H. M. (1986) *Methods Enzymol. 130*, 208−269.
26. Whitfield, J. F., Morley, P., Willick, G., MacLean, S., Ross, V., Isaacs, R. J., and Barbier, J. R. (1998) *Calcif. Tissue Int. 63*, 423−428.
27. Manning, M. C., and Woody, R. W. (1991) *Biopolymers 31*, 569−586.
28. Marx, U. C., Adermann, K., Bayer, P., Forssmann, W. G., and Rosch, P. (2000) *Biochem. Biophys. Res. Commun. 267*, 213−220.
29. Barbaro, G., Battaglia, A., Guerrini, A., Bertucci, C., and Geremia, S. (1998) *Tetrahedron−Asymmetry 9*, 3401−3409.
30. Ösapay, G., and Taylor, J. W. (1992) *J. Am. Chem. Soc. 114*, 6966−6973.
31. Gans, P. J., Lyu, P. C., Manning, M. C., Woody, R. W., and Kallenbach, N. R. (1991) *Biopolymers 31*, 1605−1614.
32. Petukhov, M., Yumoto, N., Murase, S., Onmura, R., and Yoshikawa, S. (1996) *Biochemistry 35*, 387−397.
33. Lockhart, D. J., and Kim, P. S. (1993) *Science 260*, 198−202.
34. O'Neil, K. T., and DeGrado, W. F. (1990) *Science 250*, 646−651.
35. Lyu, P. C., Gans, P. J., and Kallenbach, N. R. (1992) *J. Mol. Biol 223*, 343−350.
36. Luque, I., Mayorga, O. L., and Freire, E. (1996) *Biochemistry 35*, 13681−13688.
37. Weidler, M., Marx, U. C., Seidel, G., Schafer, W., Hoffmann, E., Esswein, A., and Rosch, P. (1999) *FEBS Lett. 444*, 239−244.
38. MacFarlane, K. J., Humbert, M. M., and Thomasson, K. A. (1996) *Int. J. Pept. Protein Res. 47*, 447−459.
39. Eisenberg, D., Weiss, R. M., and Terwilliger, T. C. (1984) *Proc. Natl. Acad. Sci. U.S.A. 81*, 140−144.
40. Sleigh, S. H., Seavers, P. R., Wilkinson, A. J., Ladbury, J. E., and Tame, J. R. H. (1999) *J. Mol. Biol. 291*, 393−415.
41. Tidor, B., and Karplus, M. (1994) *J. Mol. Biol. 238*, 405−414.
42. Prevost, M., Wodak, S. J., Tidor, B., and Karplus, M. (1991) *Proc. Natl. Acad. Sci. U.S.A. 88*, 10880−10884.
43. Maguire, P. A., and Loew, G. H. (1996) *Eur. J. Pharmacol. 318*, 505−509.
44. Swaminathan, C. P., Nandi, A., Visweswariah, S. S., and Surolia, A. (1999) *J. Biol. Chem. 274*, 31272−31278.
45. Pearce, K. H., Jr, Ultsch, M. H., Kelley, R. F., de Vos, A. M., and Wells, J. A. (1996) *Biochemistry 35*, 10300−10307.
46. Houston, M. E., Jr., Gannon, C. L., Kay, C. M., and Hodges, R. S. (1995) *J. Pept. Sci. 1*, 274−282.
47. Felix, A. M., Heimer, E. P., Wang, C. T., Lambros, T. J., Fournier, A., Mowles, T. F., Maines, S., Campbell, R. M., Wegrzynski, B. B., Toome, V., Fry, D., and Madison, V. S. (1988) *Int. J. Pept. Protein Res. 32*, 441−454.
48. Fry, D. C., Madison, V. S., Greeley, D. N., Felix, A. M., Heimer, E. P., Frohman, L., Campbell, R. M., Mowles, T. F., Toome, V., and Wegrzynski, B. B. (1992) *Biopolymers 32*, 649−666.
49. Kapurniotu, A., and Taylor, J. W. (1995) *J. Med. Chem. 38*, 836−847.
50. Pace, C. N., and Scholtz, J. M. (1998) *Biophys. J. 75*, 422−427.
51. Sreerama, N., Manning, M. C., Powers, M. E., Zhang, J. X., Goldenberg, D. P., and Woody, R. W. (1999) *Biochemistry 38*, 10814−10822.
52. Cervini, L. A., Donaldson, C. J., Koerber, S. C., Vale, W. W., and Rivier, J. E. (1998) *J. Med. Chem. 41*, 717−727.
53. Bisello, A., Nakamoto, C., Rosenblatt, M., and Chorev, M. (1997) *Biochemistry 36*, 3293−3299.
54. Condon, S. M., Morize, I., Darnbrough, S., Burns, C. J., Miller, B. E., Uhl, J., Burke, K., Jariwala, N., Locke, K., Krolikowski, P. H., Kumar, N. V., and Labaudiniere, R. F. (2000) *J. Am. Chem. Soc. 122*, 3007−3014.
55. Gekko, K., Ohmae, E., Kameyama, K., and Takagi, T. (1998) *Biochim. Biophys. Acta 1387*, 195−205.
56. Arunkumar, A. I., Kumar, T. K. S., Sivaraman, T., and Yu, C. (1997) *Int. J. Biol. Macromol. 21*, 299−305.
57. Gardella, T. J., Luck, M. D., Wilson, A. K., Keutmann, H. T., Nussbaum, S. R., Potts, J. T., and Kronenberg, H. M. (1995) *J. Biol. Chem. 270*, 6584−6588.

BI001527R